**ABSTRACT**

The present work is an attempt in predicting the performance of spring-supported thrust bearings. Thorough research has been done into the existing theories in order to incorporate them into a commercial multiphysics simulation software; COMSOL Multiphysics. The results proved the capability of coupling partial differential equations (PDE) to form a complex non linear system and thus obtaining proper results. The Reynolds equation is solved taking into account pad and collar elastic deformation and thermal expansion. The importance of including these phenomena has been evaluated. Linking the bearing material properties with the pressure and temperature developed in the assembly has been seen to play an important role.

The result of this thesis is a hydrodynamic model taking into account all the main variables involved in a spring-supported thrust bearing behaviour. The model developed could be a useful tool when designing a thrust bearing.

**AKNOWLEDGEMENT**

I would like to thank Professor Andreas Almqvist for his constant support and his ability to constantly challenge me to work out with my comfort zone.

Also thanks to Jan Ukosaari from Vattenfall who gave me the opportunity to develop this project. His regular meetings helped me to focus on the final goal and reminded me of the importance of having a good meal to work hard.

Ivar Kjelberg, Fredrik Nääs and Patrick Isaksson are some of the people who helped me when facing complex problems with the software. Esa Vuorinen helped me with the materials aspect. I would like to thank them too.

The coffee machine located in the fika room of the Machine Elements Division of Luleå University of Technology in Sweden has played an essential role during all of the Master Thesis development.

**PREFACE**

This thesis is the result of my work as a Master Student of Industrial Engineering specializing in mechanics at Luleå University of Technology. It represents the closure of my degree I started in Barcelona on 2006 and, at the same time, the beginning of the new stage of my engineering career.

The thesis has been developed under the supervision of Professor Andreas Almqvist at the Department of Engineering Sciences and Mathematics, Division of Machine Elements during the period 2012-01-16 to 2012-06-19.

F. Xavier Borràs Subirana

Luleå, June 2012

**Nomenclature**

| | |
|---|---|
| $U_r$ | $Collar\ Velocity, U_r = (u_r, v_r, w_r)$ |
| $U_f$ | $Fluid\ velocity\ field,\ U_f = (u_f, v_f, w_f)$ |
| $p$ | $Fluid\ pressure$ |
| $p'$ | $Fluid\ pressure\ corrected$ |
| $h$ | $Height\ of\ the\ gap\ /\ Fluid\ film\ thickness$ |
| $h_0$ | $Intial\ height\ of\ the\ gap/\ Intial\ fluid\ film\ thickness$ |
| $h_{min}$ | $Minimum\ height\ of\ the\ gap/\ Minimum\ fluid\ film\ thickness$ |
| $\rho$ | $Density$ |
| $\eta$ | $Viscosity\ of\ the\ fluid$ |
| $\beta_f$ | $Volumetric\ temperature\ expansion\ coefficent\ of\ the\ fluid$ |
| $E_f$ | $Bulk\ modulus\ of\ the\ fluid$ |
| $C_p$ | $Heat\ capacity\ at\ constant\ pressure\ of\ the\ fluid$ |
| $k$ | $Thermal\ conductivity$ |
| $k_p$ | $Thermal\ conductivity\ of\ the\ pad$ |
| $k_r$ | $Thermal\ conductivity\ of\ the\ collar$ |
| $k_f$ | $Thermal\ conductivity\ of\ the\ fluid$ |
| $x, y, z$ | $Cartesian\ coordinates\ system$ |
| $r, \theta, z$ | $Cylindrical\ coordinates\ system$ |
| $\omega$ | $Angular\ velocity\ of\ the\ collar$ |
| $\tau$ | $Tangencial\ forces$ |
| $n_{pads}$ | $Number\ of\ pads\ in\ the\ thrust\ bearing$ |
| $\varphi$ | $Inclination\ of\ the\ gap$ |
| $\varphi_x$ | $Inclination\ of\ the\ gap\ in\ x\ direction$ |
| $\varphi_y$ | $Inclination\ of\ the\ gap\ in\ y\ direction$ |
| $He$ | $Piecewise\ function\ to\ correct\ the\ negative\ pressures$ |
| $e$ | $Boundary\ value\ of\ the\ piecewise\ function\ to\ correct\ the\ negative\ pressures$ |
| $u$ | $Deformation\ in\ x\ direction$ |
| $v$ | $Deformation\ in\ y\ direction$ |
| $w$ | $Deformation\ in\ z\ direction$ |
| $W_{ext}$ | $External\ load$ |
| $F_{fluid}$ | $Integral\ of\ the\ fluid\ pressure\ on\ the\ pad\ surface$ |
| $E$ | $Young's\ Modulus$ |

$E_p$ $Young's\ Modulusof\ the\ pad$

$E_r$ $Young's\ Modulus\ of\ the\ collar$

$E_{eq}$ $Equivalent\ Young's\ Modulus\ pad-collar$

$E_s$ $Equivalent\ Young's\ Modulus\ of\ the\ pattern\ of\ springs$

$\upsilon$ $Poisson's\ ratio$

$\upsilon_p$ $Poisson's\ ratio\ of\ the\ pad$

$\upsilon_r$ $Poisson's\ ratio\ of\ the\ collar$

$\upsilon_{eq}$ $Equivalent\ Poisson's\ ratio\ pad-collar$

$\alpha_L$ $Coefficent\ of\ thermal\ expansion$

$\alpha_{L_p}$ $Coefficent\ of\ thermal\ expansion\ of\ the\ pad$

$\alpha_{L_r}$ $Coefficent\ of\ thermal\ expansion\ of\ the\ collar$

$\sigma$ $Normal\ stress$

$\Delta h_B$ $Height\ variation\ due\ to\ the\ collar\ deformation$

$\Delta h_T$ $Height\ variation\ due\ to\ the\ tilting\ of\ the\ pad$

$\Delta h_W$ $Height\ variation\ due\ to\ the\ pad\ deformation$

$\delta$ $Springs\ elongation$

$k_s$ $Elastic\ constant\ of\ the\ spring$

$k_{s_e}$ $Equivalent\ elastic\ constant\ of\ the\ pattern\ of\ springs$

$F_s$ $Force\ of\ the\ springs$

$L_A$ $Distance\ to\ the\ pivot\ point$

$L_{A_x}$ $Distance\ to\ the\ pivot\ point\ in\ x\ direction$

$L_{A_y}$ $Distance\ to\ the\ pivot\ point\ in\ y\ direction$

$n_s$ $Number\ of\ springs$

$A_s$ $Area\ of\ the\ springs\ equivalent\ volume$

$d_s$ $Height\ of\ the\ springs\ equivalent\ volume$

$L_s$ $Location\ of\ the\ spring$

$L_{s_x}$ $Location\ of\ the\ spring\ in\ x\ direction$

$L_{s_y}$ $Location\ of\ the\ spring\ in\ y\ direction$

$T$ $Temperature$

$T_f$ $Temperature\ of\ the\ fluid$

$T_p$ $Temperature\ of\ the\ pad$

$T_r$ $Temperature\ of\ the\ collar$

$T_b$ $Temperature\ of\ the\ bath\ of\ fluid$

$T_{lead}$ *Temperature of the fluid in the leading edge*

$T_{trail}$ *Temperature of the fluid in the trailing edge*

$\beta_p$ *Angular extension of the pad surface*

$r_i$ *Inner radius*

$r_o$ *Outer radius*

$N$ *Pad thickness*

$A_{pad}$ *Area of the pad surface*

$A_{step}$ *Area of the step surface*

$A_{groove}$ *Area of the groove between pads*

$Q$ *Heat tranfer*

$Q_{vh}$ *Heat generated due to the viscous heating*

$Q_l$ *Side leakage heat transfer*

$Q_r$ *Heat transfer through the runner*

$Q_p$ *Heat transfer through the pad*

$Q_g$ *Heat transfer through the groove between pads*

$P_b$ *Heat Loss in the pad*

$q_r$ *Fluid flow rate in r direction*

$q_\theta$ *Fluid flow rate in θ direction*

$H$ *Convective heat transfer coefficient*

$H_p$ *Convective coefficient between the fluid and the pad lower surface*

$H_l$ *Overall convective coefficient fluid − lower surface of the pad*

$H_u$ *Coefficent between fluid and collar*

$Ur$ *Coefficent between fluid and collar including the size factor*

$\delta_{def}$ *Centre to edge dflection of the pad*

$k_c$ *Factor conditioning the pressure applied on the collar*

$s$ *Collar preload deformation parameter*

# Table of Contents

# 1 Introduction

*Cease from grinding, ye women who toil at the mill;*
*Sleep late, even if the corwning cocks announce the dawn.*
*For Demeter has ordered the Nymphs to perform the work of your hands,*
*And they, leaping down on the top of the wheel, turn its axle which,*
*With its revolving spokes, turns the heavy concave Nisryan millstones,*
*Learing to feast on the products of Demeter without labour.*

*Antipater of Thessalonica (year 15 BC)*

The use of flowing water to generate mechanical movement has played an important role along the history. The Egyptians and later the Persians were the firsts to take advantage of such a useful energy source. Turbines were first used to ease the grain milling task. However, the Egyptians could never have imagined what the scope of their discovery was.

These early turbines were commonly made with timber and the shaft, usually a tree trunk, was handled on some support as rocks or some wooden structure. An important part of the energy was wasted on the friction between those surfaces; the rotational velocity was low enough to do not worry about it. In fact, water movement was used to generate work, so water turbines were born.

These hydro powered machines have been improved along the years since people realized that this mechanical energy obtained was more useful as electricity. However, the mechanical stage is nowadays still inevitable.

Hydroelectric power has been used for many centuries. The components involved such as blades, axis, and bearings have been improved in order to achieve a better efficiency. The contact pair between the spinning axis and the fixed part that handles the shaft is an essential piece of the turbine.

All energy generating machines shares the same final goal; to produce as much energy as possible. Therefore -to increase the amount of energy obtained- bigger sources were found involving the need of bigger machinery. Due to the huge dimensions of the axis, the load handled by the bearing also turns huge. Bearings prepared to carry high axial loads are needed. The thrust bearings handle huge axial loads [1] and also allow the shaft to rotate at the required angular velocity.

The main feature of these thrust bearings is to provide for separation between the shaft and the support, something essential when working with hundreds of tones spinning at hundreds of revolutions per minute. A physical contact between both surfaces would mean the destruction of the machine. A highly pressured, micrometre thin, lubricant film is located between the collar or runner (mobile part) and the pad (fixed part). The static piece is compound from a number of segment shaped pads. All the different kinds of thrust bearings have in common to provide for the absence of mechanic contact between the dynamic and the static part.

When it comes to support the highest pressures, it is known that the inclination of the pads plays an important role. The angular velocity of the collar shears the lubricant into the convergent clearance between the pad and the collar. This generates a non-negligible pressure distribution on both pad and collar. Varying the inclination of the pads, this pressure distribution can be adjusted to increase the load carrying capacity, modifying the film thickness and possibly improving the efficiency. So the geometry and the inclination of the pad is a significant point of study.

The most common type of thrust bearings for hydropower applications are the tilting pad thrust bearings (TPTB). In this kind of thrust bearings, each pad is placed over a spherical pivot that allows tilt to the surface. However, a fixed defined pivot point restricts heavily the freedom degrees of the pad. Thorough research was done to figure out the proper location of the pivot point in order to improve the bearing behaviour. Although TPTB allows, theoretically, the optimum inclination of the pad under certain conditions, it restricts the range of working conditions. In addition, many variables difficult to take into account are involved in a thrust bearing performance, so there is a high grade of ignorance that generates some doubts about the accuracy of an optimum pivot point position. TPTB also have many problems on the contact point between the pad and the lower surface. Due to its punctual contact point and the huge external load to bear, the pressure on this point is extreme. A variant from TPTB are the discs thrust bearings, the pad slides over a circumferential profile increasing this way the area of the pivot and therefore reducing the pressure to bear.

To work with even higher loads, the pads supported on a punctual pivot point are not enough. The pressure on that pivot becomes too high. To allow tilting and at the same time avoid the punctual contact, the spring-supported thrust bearings were created. The pads lie on a spring mattress that handles the applied load. The springs-supported thrust bearing has good self adjustment and heat dissipation. It is also of benefit with respect to vibration in running [2].

It is well-known the argument between tilting-pad and spring-supported thrust bearings supporters. It is not clear which grants better results. Although the spring-supported has a not defined pivot point, the spring pattern hampers considerably its study.

This thesis goes further in the performance of the spring-supported ones.

Multiphysics modelling of a spring-supported thrust bearing has been carried out in order to understand the relevance of considering some different parameters when designing, easing this way the prediction of thrust bearings performance. The first part of the study is common for all kinds of thrust bearings and then it comes closer to the spring-supported one of the study case.

The analysis of thrust bearings is varying from using exclusively finite differences methods to a mix between theses ones and FEM. This study implements the thrust bearing model in the commercial multiphysics modelling software COMSOL Multiphysics. This software utilise the finite element method (FEM) to discretize the system of partial differential equations, constituting the multiphysics model of the thrust bearing and a substantial computational effort is required for the simulation to converge to specific tolerances.

The complexity of this study is mostly the strong linkage between all the phenomena involved from different engineering fields. The variation of a single variable implies a completely different performance that will also affect the modified variable in the following iteration. Even more difficult than defining the PDE equations system is to the design the path that leads to a convergent solution. Another tough part is to specify the boundary conditions when solving the complex coupled PDE system due to the lack of generalised data available. The most part of the studies, due to its difficult physical approach, is to adapt the multiphysics model to match the simulation results with the experimental ones. That limits considerably the task of designing a global model for every thrust bearing.

The present study carried out is a thermoelastohydrodynamic analysis (TEHD) which requires a high computational capacity to solve complex FEM systems. For its facility of coupling different physic phenomena, COMSOL Multiphysics has been chosen as the software to handle the simulation. The main advantage of COMSOL Multiphysiscs is that it allows working with PDE expressions making it possible to study advanced mathematical systems. This software also eases importing models and expressions from Matlab. The drawback of COMSOL Multiphysics is the need of defining accurately the conditions applied and seed values in order to get a solution. The absence of well defined conditions turns simulations into a time consuming computing process that ultimately leads to a non-convergent solution and an error message from the simulation software. This complicates the implementation of the model.

The study is focused on the elastic deformation produced on both pad and collar as a consequence of the pressure on the lubricant and also the thermal expansion induced by the temperature rise due to the viscous heating. The elastic deformation modifies the shape of the clearance between surfaces which in turn affects the pressure distribution. Thermal effects have been also considered in order to achieve a model as capable to predict the real working conditions. The importance of including the thermal effects, via the energy equation, within the fluid domain and the heat equation in the pad and the collar, has been demonstrated. It is shown, that the results without taking into account the thermal effect are completely different from those that do. Thermal expansion seems to be as important as the elastic deformation. These results point out the importance of considering the non-stationary nature of operation found in real machines. In the present model, the steady-state temperature is gradually reached through the non-steady state and the sagging produced by the pressure is gently compensated by the thermal expansion giving this way rise to the well-documented crowning effect [3]. Also the variation with temperature and pressure of some proprieties, especially viscosity, has been assessed.

# 2 Objectives of the Thesis

This work is based on the study of an already running spring-supported thrust bearing from a hydroelectric plant located in Norrbotten (Sweden). This thrust bearing has been working for 50 years under certain conditions; however these conditions are far from the original design intention. Although the turbine has and still is working fine, its behaviour worries the company in charge for possible unexpected effects. Working under unexpected conditions can produce unexpected consequences; the company wished to ensure the safety of the employees by making the turbine operate under controlled conditions. This study has been carried out with the objective of developing and implementing a generalized multiphysics model for this particular spring-supported thrust bearing. The final aim it to make use of this model to study the effects of a number of parameters on bearing performance.

The study carried out, done half a century after the turbine installation, has as a first goal to simulate a working thrust bearing including as many relevant variables as possible. Secondly, it tries to figure out which can be the cause of its unexpected behaviour. This is a difficult task, as it is not possible to use the experimental data from the actual bearing to adjust the model.

The study has been scheduled in order to develop, step by step, the multiphysics model to more and more accurately simulate the real pad. This methodology ensures reliable results, which is extremely necessary since there is a lack of experimental data to validate the model against in this case. Although there are a number of articles on thrust bearings, it is difficult to obtain anything more than some guidelines helping to verify that the results follow the expected tendency.

Each step has the complexity of understanding to how to model the physics and, after that, figure out the proper way to input it in the simulation software.

Unfortunately, there are many factors that affect the behaviour of the elements from a thrust bearing during operation. Despite this, the working plan was to gradually add the physics from the most important to the less important one. What makes this study interesting is the interdisciplinary nature, coupling different physic fields such as thermodynamics and hydrodynamic.

Due to the lack of studies considering so many phenomena to predict the bearing performance, the objective of the thesis is also to verify the importance of the variables added into the FEM model. It is interesting to be aware of the importance of including or not some specific variable into the simulation. Each variable included heavily increases the computational effort required and thus it increases the time needed for every simulation.

# 3 Summary of Literature Survey

*"In fact is very hard to think of any moving system where there is both a wedge and a velocity in two perpendicular directions. A tilted sleeve bearing along a rotating shaft would qualify but it is likewise not easy to imagine a useful machine round such a device."*

*Alastair Cameron, Basic Lubrication Theory*

There are many studies related with thin lubricant films located between two sliding surfaces. An important part of the Tribology research deals with lubrication on bearings. The most part of the lubrication theories are based on the work of Osborne Reynolds [4], who is considered the father of the science of hydrodynamic lubrication. The theory provides insight into the behaviour of thin lubricant films.

For its wide range of applications, journal bearings have been extensively studied. However, papers focused on thrust bearings and in particular on spring-supported ones, are not so common. The approach to modelling and simulating of thrust bearings has changed from its origins to this date. In the beginning, finite difference methods were used for simplicity. Nowadays there is the tendency of moving towards the finite element method. This has become feasible due to the computational resources nowadays available.

Sternlicht was among the first to publish solutions coupling the Reynolds and the energy equation. His team realized the importance o role the temperature is playing in the bearings performance. He also noticed that the inlet temperature, i.e., the temperature of the oil passing over the leading edge was a key parameter and that this temperature was heavily influenced by the oil/gas mix produced in the groove between pads [5]. His study considered a 2D plane lubricant film. In the same conference he exposed his results the first THD description of the oil film in elevation was given by Zienkiewicz [6].

Later Rothbar confirmed that the surface pressure gets smaller increasing its deformation. Less pressure on the surface means a decrease on load carrying capacity [7]. In 1963 Dowson and Hudson gave 2D elevation solutions (solving it for a unique radius; not considering the depth in the radial direction) for the film components [8]. Although 2D elevation solutions give a better approach of the heat flow in a bearing, plane solutions (considering the variables constant along the height) were deeply studied for the following two decades.

Ettles is a scientist who has dedicated an important part of his efforts to the study of thrust bearings. He introduced the concept of hot oil carry-over effect while he was studying the fluid behaviour in the grooves between pads [9] [10].

The best approach solving the Reynolds equation on a two dimensions model was achieved by Castelli and Maloski [11]. However, lately it has been seen that 3D models were, in many cases, needed to achieve useful results.

Another researcher focused on predicting thrust bearings operating temperatures is J. H Vohr. He introduced the idea of an energy balance approach via a control volume that includes the entire pad. He adjusted the heat transfer coefficients of each surface to match

with experimental data. In [12] Vohr suggests that Ettles' solution may not properly address the thermal effects and ensured that his energy balance obtains more accurate prediction. His study has been a reference for the most part of the recent researchers focused on the temperature distribution in thrust bearings.

In 1982 Ettles presented a method for the temperature calculation in the thrust bearing assembly. The method included reverse flow phenomenon and simplifies the hot oil carry-over calculation. Some importance was given to the transient thermo elastic effects [13].

A few years later, Ettles presented a new paper describing techniques to get even better transfer heat coefficients [14]. In this paper he does a good overview of 2D and 3D methods for thrust bearing analysis. A method to solve the troubles that appear when adding a third dimension to the model is explained. He also points out the advantages of using "double layer" pads, i.e., a thin plate layer is mounted on the pad of regular thickness. The chamfer on the plate takes advantage of the velocity ram effect to boost the flow. It also improves the heat dissipation decreasing the operating temperatures.

Heshmat and Pinkus presented a paper about the mixing inlet temperatures in the groove [15]. They coupled the finite difference and finite element methods in an iterative process to model gas lubricated thrust bearings. They stated that the load carrying capacity can be steadily increased by reducing the film thickness.

Dimarogonas pointed out the importance of uncertain variables such as the machining accuracy or the thermal and mechanic distortions of the surfaces under working conditions as sources that limits confidence of theoretical results [16].

The hydrodynamic effects of thrust bearings on the statics and dynamics of a rotor-bearing system were studied by Jaing and Yu [17]. They stated that the action of the thrust bearing has two limits one in static state (machine is stopped) and another one in dynamic state (when the shaft is rotating). Mittwollen et al. carried out research on the influence of lateral vibrations from hydrodynamics thrust bearings on the dynamics characteristics of the total rotor system [18]. Neither the hydrostatic behaviour nor the vibrations are considered in the present work.

Ettles published another paper discussing the effects of pad size and springs arrangement on its behaviour by thermoelastohydrodynamic analysis [19]. He improved Vohr's treatment adding a shear correction calculation using a conventional finite difference method.

Ashour paid special attention to the elastic distortion on spring-supported thrust bearings [20]. Shina also did a thorough research on the same field [21].

Gardner went deeper into the linkage between bearing power loss and pad operating temperatures on the oil flow. The importance of the temperature distribution on thrust bearings behaviour and its effect on the other variables as the load carrying capacity were pointed out [22]. Ferguson continued studying the importance of oil viscosity and its relevance on the power loss from spring-supported thrust bearings. Using the specialized software GENMAT and comparing the results with experimental data obtained showed

that considerable energy savings could be achieved by lowering the oil viscosity, especially for large pad bearings [23].

In 1999 Wang reported on the effects of different spring patterns and pad stiffness as well on spring-supported thrust bearings taking into account pad thermo-elastic distortion [24]. The same year Storteig and White finished their work on fast computational routines to evaluate the main dynamic coefficients for hydrodynamically lubricated tapered land bearings [25].

In 2001 Brown and Medley went further on the limits on hydrodynamic lubrication at low rotor speeds. At low angular velocities the lubrication is basically hydrodynamic rather than thermodynamic. They also did some statement about the surface roughness of the pad [26].

Up to this point, pad deflection was generally treated via finite difference methods. The biharmonic plate bending equation was used adding some modifications to include thermal effects and springs behaviour.

One year later, Brown presented another paper with a good approach of spring-supported thrust bearings including hydrostatic and hydrodynamic lubrication. He left behind the biharmonic plate bending finite differences method to calculate the deformation of the pad. Using full structural mechanics and FEM, he was able to include different material layers on the pad and also model the springs without violating the thin plate assumptions. The model considers isothermal fluid flow [26]. The same method for solving pad deflection has been used in the following study. The springs where fully modelled underneath the pad assuming its deformation could be matched with the springs contraction. A thin plate has been also modelled. Different material proprieties were allocated to the pattern of "springs", the pad and the thin plate.

This same year, Sergei Glavatskih published a paper explaining how to measure simultaneously the oil film thickness and the temperature on fluid film bearings [27].

Osman used a combination between finite difference methods and FEM to solve Reynolds Equation, Energy Heat Conduction and thermo-elastic expressions. The results were compared with data obtained from empirical experiments that he also carried out. It was shown that thermo-elastic deformation plays an important role [28]. They also studied the importance of several other factors, such as the spring pattern, the pad thickness and the initial pad geometry.

In [29], Markin reported on FEM simulations of tilting-pad thrust bearings considering both surfaces pad and runner using an intermediate layer to model the lubricant. This is the only paper which considers the pad and the runner deformations separately.

Michal Wasilczuk compared the efficiency of different supply methods in [30]. As it is stated, the inlet temperature is one of the main parameters in the analysis of fluid film bearing performance. Wasilczuk's paper focused on the role of the groove between pads and its effectiveness when supplying new cold lubricant.

First Toklar and then later Güllu [31] verified the importance of bearing deformations considering a rigid collar. Later Karadere [32] developed a comparative study between different gap definitions when solving the Reynolds equation. The results between including the deformation of pad, the deformation of both pad and runner and no deformation on the surfaces were discussed.

Srikanth [33], focused his study on the angular stiffness of large tilting pad thrust bearings. The FEM model they developed solves Reynolds' equation for pressure and the energy equations and temperature distribution across the film. Their model takes viscosity variation and hot oil carry-over into account, using Ettles' assumptions. The present work shares the same goal; to achieve a good FEM model that is able to predict the running conditions of spring-supported thrust bearings.

According to the author's knowledge, there exists no model in the literature that considers pad tilt as a dependent variable and solves the problem to predict its value. The papers that address variation of pad inclination, introduce a parameter describing the inclination, then vary this parameter and study its influence on load carrying capacity, friction force, etc.) [20] [21] [25] [28] [32] [33]. However, the pad inclination is not usually known while running therefore the former approach is to be preferred. In addition, after including the thermal expansion, this work shows the surfaces are not flat so the only feasible way of considering the tilt of the pad is by modelling it as a dependent variable someway. In the present work, the pad is modelled as an elastic body supported by an array of elastic cylinders, representing the spring support of the actual bearing that this work focus on.

The collar (or runner) is as well considered as being an elastic body that exhibits mechanical as well as thermal deformations, dependent on simulated operating conditions. During the solution procedure, the pad then flexes and tilts to fulfil the specified force and moment equilibrium equations. In addition, an auxiliary 3D fluid domain is introduced as a solution domain for the energy equation describing heat conduction and convection within the fluid film.

# 4 Method

The study has been focused around the pressure exerted on the pad by the fluid due to the important role that plays when studying thrust bearings. It is also the most complex issue when solving the system. The Reynolds equation is the one which fits better with the behaviour of the thin lubricant layer located between pad and runner. It enables to determine the pressure distribution in a bearing with an arbitrary film shape [29]. So the main goal of this project has been to solve the Reynolds partial differential equation, under well-defined conditions. The study started with the most basic form of the equation, then additional physics have been introduced step-by-step to verify the model for each new effect studied.

During the course of the project, the solution procedure was modified several times. However, the working strategy has been always the same one: do not add additional physics until the previous stage has been properly verified. For example, the thermal effects were not considered until a proper pad deflection model was obtained. A selection of physic effects is considered based on their importance to approach the final goal: a close prediction of the behaviour of a spring-supported thrust bearing. The problem solving methodology followed was defined by the literature review.

Three main physics were selected to be included in the model. They have been considered in following order:

I) Pressure distribution
II) Solid mechanics; elastic deformation
III) Thermal effects; expansion and formation

The main computational structure developed to numerically solve the thrust bearing problem at hand, turned out to be similar to the one proposed by Markin [29].

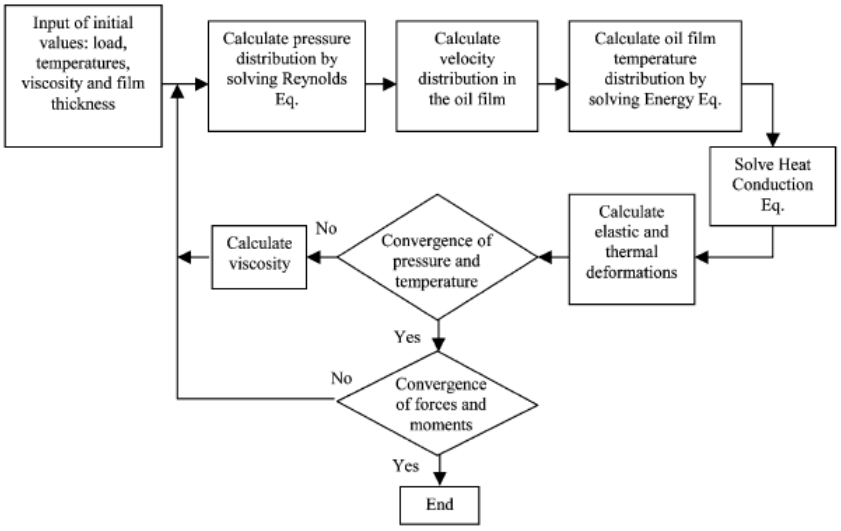


*Figure 1. Data flow chart of the software computation [29].*

Markin analysed the performance of a tilting-pad thrust bearing solving the two dimensions Reynolds equation applied on the pad surface of his 3D model. It is the only paper found which considers the entire thrust bearing assembly (pad, lubricant layer and collar) at the same time. This is also the reason why its data flow chart resembles the one in the present study.

## 4.1 Pressure Distribution

The relative movement between two surfaces separated by a thin layer of fluid generates a lubricant velocity field and consequently a non-negligible pressure distribution acting on both surfaces is found. It is the pressure distribution that balances the weight of the enormous shaft and the turbine, found in hydropower generating plants with a Kaplan or Francis turbine assembly.

### 4.1.1 Navier-Stokes Equation

The Reynolds equation is a simplified subset of the Navier-Stokes equation *(Eq. 1)*. When analysing a thin lubricant flow Reynolds equation is commonly used for its practical application while Navier-Stokes full equations are used to find validity limits of Reynolds equation. Both methods give similar results when working with narrow gaps, however when the minimum distance of the channel throat is increased the pressure values obtained become quite different [34].

$$\rho \cdot \left( \frac{\partial U_f}{\partial t} + U_f \cdot \nabla U_f \right) = -\nabla p + \nabla \cdot \bar{T} + f \qquad (1)$$

It is assumed that the fluid flow between pad and collar is never turbulent and the model applied is only valid for laminar fluids. It is a common assumption although it is known that turbulent flow exists under certain points of operation [35]. The transition from laminar to turbulent flow occurs at the leading edge first where the fluid flow is thicker.

Although it is known that the results would be more accurate using the full Navier-Stokes equations, the complexity of the calculations is increased heavily. So the Reynolds equation *(Eq. 2)* has been used for the thin lubricant film calculations as nearly all of the available papers do.

The Reynolds equation adopted for this study reads:

$$\nabla \left( \frac{\rho h^3}{12\eta} \nabla p \right) = \frac{U_r}{2} \nabla (\rho h) \qquad (2)$$

The fluid density $\rho$ and the viscosity $\eta$ are really significant. To obtain desired pressure $p$ it is often easier to switch the lubricant type instead of modifying other parameters as the gap height $h$ or the relative motion between surfaces, which in this case is identical to the collar velocity $U_r$. The other variables are related to the fluid.

### 4.1.2 Reynolds' equation in 1D

Initially, the problem connected to the flow in an infinitely wide convergent gap is treated; see also Dowson et al. [8]. The schematic of the presumed bearing is displayed in *Figure 2*.

The Reynolds Equation describing a compressible flow in one dimension is:

$$\frac{d}{dx}\left(\frac{\rho h^3}{12\eta}\frac{dp}{dx}\right) - \frac{U_r}{2}\frac{d}{dx}(\rho h) = 0 \qquad (3)$$

Where $\rho$ is the lubricant density, $\eta$ is the viscosity, $U$ is the collar velocity and $h$ is the gap defined between pad and collar geometry. At the beginning of this project, a model for an isothermal, incompressible and isoviscous lubricant was studied. In terms the parameters in the Reynolds equation, this may be expressed as:

$$\rho = \rho_0 \;\; \eta = \eta_0 \qquad (4)$$

Initially, as it is seen in *Figure 2*, it is also assumed that pad and collar are rigid so there is no deformation on their surfaces, which means that the gap geometry only depends on $x$, i.e.:

$$h = h(x) \qquad (5)$$

Since slip at the surface is not considered, the fluid next to the surface has the same velocity as the wall in contact. That means that there is a fluid velocity gradient from the fluid layer in contact with the pad and the film next to the collar, moving at the same velocity as the shaft.

The boundary conditions required to get a unique solution from the PDE are that the pressure on the edges must be the atmospheric one. This is mathematically expressed by the following Dirichlet boundary conditions:

$$p(0) = 0 \qquad p(L) = 0 \qquad (6)$$

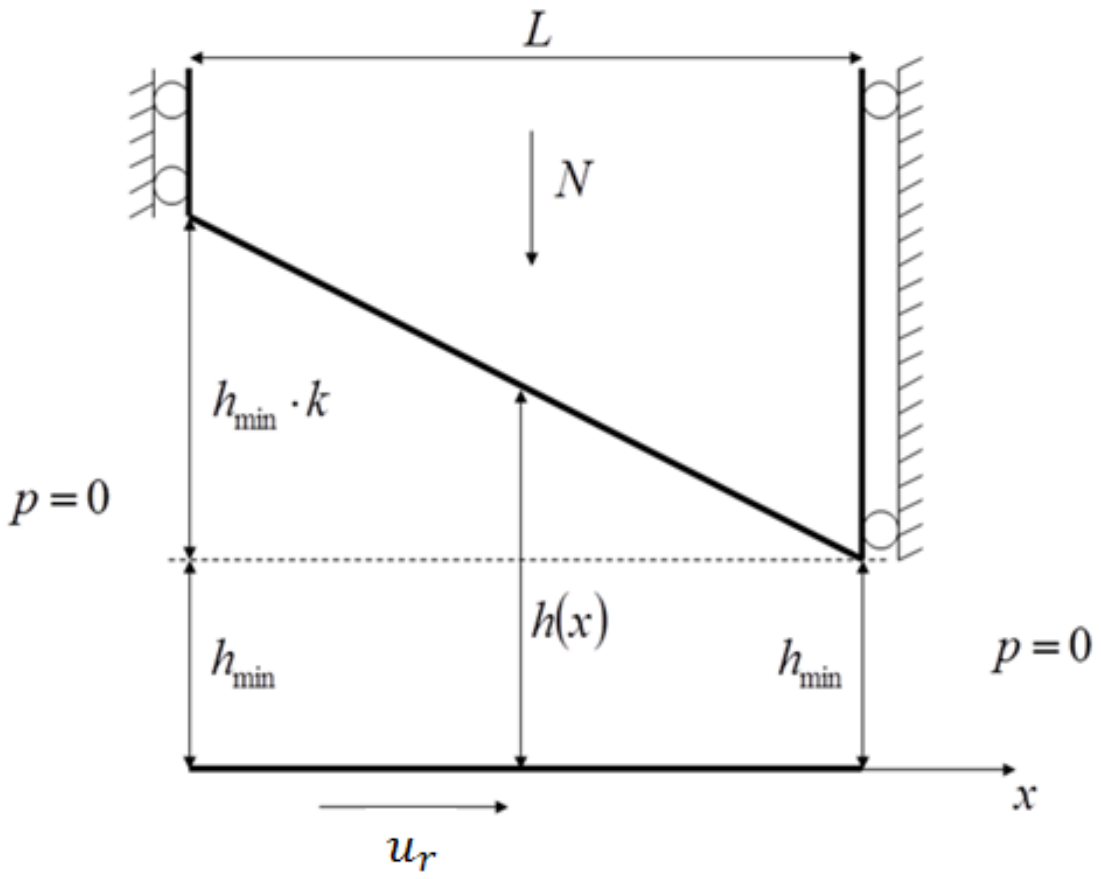


*Figure 2. Gap geometry and boundary conditions.*

From *Figure 2*, it is clear that the film thickness (the gap between the moving plane and the stationary wedge type of bearing) is:

$$h(x) = h_{min} \cdot (1 + k - \frac{k}{L} \cdot x) \quad (7)$$

Where the parameter $k$ is given by:

$$k = \tan(\varphi) = \frac{h_{max} - h_{min}}{h_{min}} \quad (8)$$

By varying the pad inclination angle, $\varphi$, while keeping the wedge in a fixed position ($N$ will thus vary), different pressure distributions (profiles) are achieved. As shown in *Figure 3*, a small variation of the tilting angle $\varphi$ imposes a significant change of the pressure distributions.

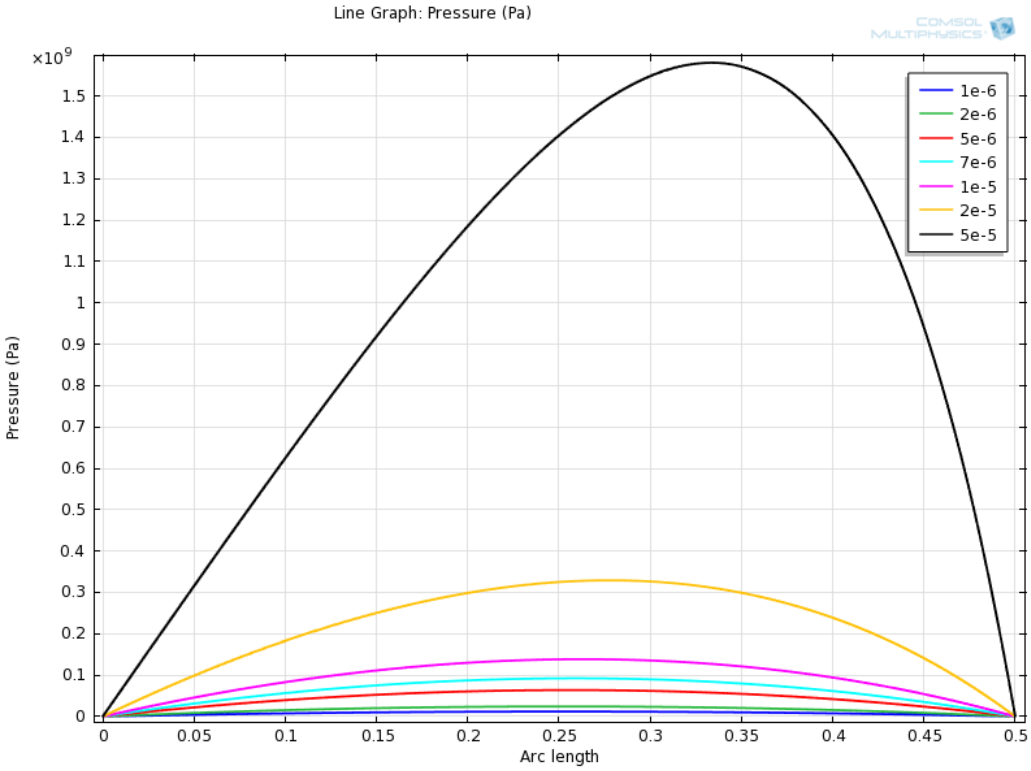


*Figure 3. Inclination φ Sweep.*

As it is seen in the figure, the pad must carry extreme pressures. Due to the magnitude of the pressures, the materials from the pad and the collar must be carefully selected. This pressure distribution is assumed constant, however, in real life; the pressure is slightly variable. The vibration of the machine is heavily reduced by using spring-supported pads instead of the tilted pad ones.

### 4.1.3 Reynolds' equation in 2D

Ettles described in one of his early papers the importance of considering the third dimension when studying thrust bearings [14]. He also gave some tips to solve the problems that appear when implementing a 3D thrust pad bearing simulation.

For a 3D geometry the Reynolds equation is a two dimensional PDE. Under stationary conditions the Reynolds equation describing compressible flow reads:

$$\frac{\partial}{\partial x}\left(\frac{\rho h^3}{12\eta}\frac{\partial p}{\partial x}\right)+\frac{\partial}{\partial y}\left(\frac{\rho h^3}{12\eta}\frac{\partial p}{\partial y}\right)=\frac{U_r}{2}\frac{\partial(\rho h)}{\partial x} \qquad (9)$$

A comparative study between the 2D and 3D models has been carried out in order to check the necessity of considering the second dimension when modeling spring-supported thrust bearings, but also to verify the implementation of the 3D model.

The 1D Reynolds solutions can be used when treating with pads with large width (compared to the length of the pad) [36]. In order to justify the correctness of the solution of the Reynolds Equation in two dimensions, the pressure distributions obtained are compared with the ones obtained for the 1D problem.

The width of the pad and the pad inclination was varied according to *Table 1* to evaluate the influence of considering a second dimension.

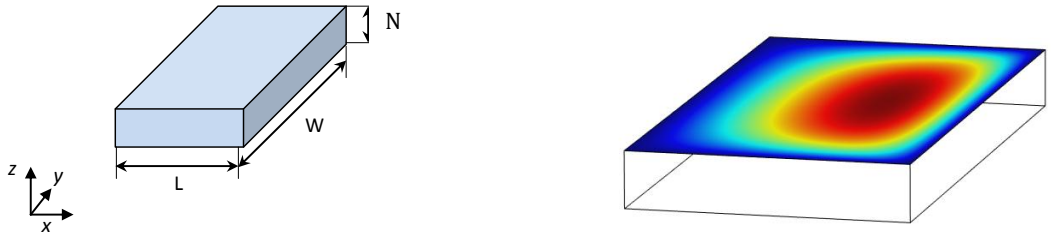


*Figure 4. Pad dimensions parameters and pressure distribution.*

| Pad Inclination $\varphi$[rad/s] | 1 Dimension Max Pressure [MPa] | 2 Dimensions Max Pressure [MPa] | | | |
|---|---|---|---|---|---|
| | W = 0 [m] | W = 10 [m] | W = 5 [m] | W = 1 [m] | W = 0,5 [m] |
| **1E-6** | 1,20 | 1,20 | 1,20 | 1,09 | 0,71 |
| **2E-6** | 2,44 | 2,44 | 2,44 | 2,23 | 1,44 |
| **5E-6** | 6,39 | 6,39 | 6,39 | 5,83 | 3,77 |
| **7E-6** | 9,23 | 9,23 | 9,23 | 8,42 | 5,45 |
| **1E-5** | 13,86 | 13,82 | 13,82 | 12,63 | 8,18 |
| **2E-5** | 32,91 | 32,51 | 32,65 | 30,03 | 19,55 |
| **5E-5** | 158,03 | 157,76 | 156,96 | 145,72 | 99,47 |

*Table 1. Comparison between considering Reynolds equation in 1D or in 2D (L=0, 5 [m], U (x-direction) = 1 [m/s], N= 0, 1 [m]).*

The results, taking the maximum pressure as the reference value, showed the goodness of considering an infinite pad (1D Reynolds Equation) for wide pads. However, when the width of the pad is approaching the length of the pad, the results become significantly different, showing the necessity of applying the two dimensional Reynolds equation for the present work.

### 4.1.3 Collar Angular Velocity

Cartesian coordinates $(x, y, z)$ have been used to define the geometry of the pad and the physics applied.

As the pad is a segment shaped piece with radial symmetry, it is important to consider the possibility of using a cylindrical coordinates system $(r, \theta, z)$. It is admitted that the velocity field or the pad geometry would be much easily to define. Despite that, the wall inclination or the rounded corners on the pad surface turns to be a tough job. In addition, COMSOL Multiphysics software has much better results working with $x$, $y$ and $z$ coordinates. However, the most part of scientific papers related with thrust bearings approach the problem by using cylindrical coordinates due to the simplified pad geometry they assume.

Turbines, as rotor machines, rotate around an axis, so the problem faces an angular velocity distribution $\omega$. The linear velocity $U$ of each point of the collar increases linearly with its distance to the rotation axis $r$.

$$U_r = \omega \cdot r \qquad (10)$$

This distance $r$ is defined as,

$$r = \sqrt{x^2 + y^2} \qquad (11)$$

The velocity is perpendicular to its radius so, in order to fit it into a Cartesian coordinates system $(x, y, z)$, it is trigonometrically decomposed in a certain angle $\theta$ (*Figure 5*).

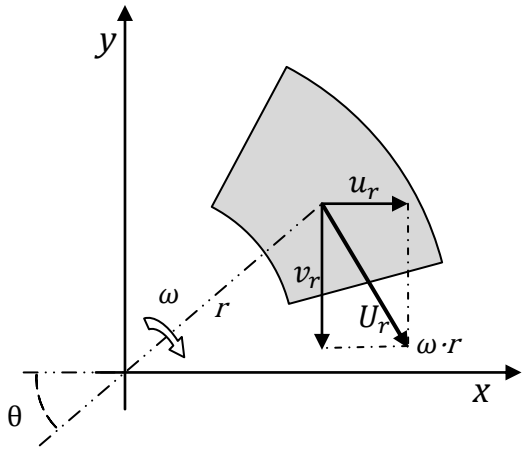


*Figure 5. Angular velocity trigonometric decomposition.*

Taking into account that the turbine rotates in a clockwise direction viewed from above, the velocity field expression in Cartesian coordinates is:

$$u_r = \omega \cdot r \cdot sin\,\theta \qquad (12)$$
$$v_r = -\omega \cdot r \cdot \cos\theta \qquad (13)$$
$$w_r = 0 \qquad (14)$$

### 4.1.4 Fluid Film Velocity Field

The fluid velocity field generated due to the relative movement between the pad and runner surfaces plays an important role for thrust bearing performance. The velocity field is deduced considering the following method.

Considering an infinitesimal friction model, such as depicted in *Figure 6*.

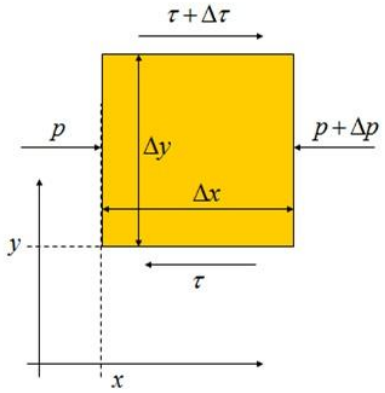


*Figure 6. Infinitesimal friction model.*

local force equilibrium can be formulated according to:

$$(\tau + \Delta\tau) \cdot \Delta x - \tau \cdot \Delta x + p \cdot \Delta y - (p + \Delta p) \cdot \Delta y = 0 \Rightarrow$$

$$\frac{\partial \tau}{\partial y} = \frac{dp}{dx} \qquad (15)$$

if inertia is neglected. The lubricant is assumed to behave as a Newtonian fluid, so in other words, it i.s a fluid whose stress versus strain rate curve is linear and passes through the origin [37].

$$\tau = \eta \cdot \frac{\partial U_f}{\partial y} \qquad (16)$$

This can be rewritten as:

$$\eta \cdot \frac{\partial {U_f}^2}{\partial y^2} = \frac{\partial \tau}{\partial y} \qquad (17)$$

Together with the relationship between shear stress and fluid pressure *(Eq. 15)*, the velocity field dependent on the pressure distribution, can be obtained:

$$\eta \cdot \frac{\partial {U_f}^2}{\partial y^2} = \frac{\partial p}{\partial x} \qquad (18)$$

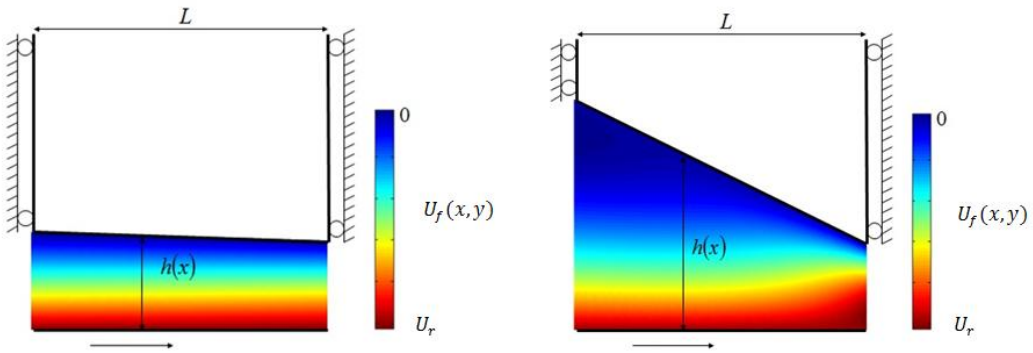


*Figure 7. Fluid velocity fields for different gap profiles.*

In *Figure 7*, the velocity field for two different bearing configurations has been plotted. It is appreciable by first solving the 1D Reynolds equation for the fluid pressure and then integrating *Eq. 16* twice with respect to $y$.

Following this procedure, the fluid velocity field $U_f$ is obtained,

$$\frac{\partial}{\partial x}\left(\frac{\rho h^3}{12\eta}\frac{\partial p}{\partial x}\right)+\frac{\partial}{\partial y}\left(\frac{\rho h^3}{12\eta}\frac{\partial p}{\partial y}\right)=\frac{\partial}{\partial x}\left(\frac{u_r}{2}\left(\frac{\partial(\rho h)}{\partial x}\right)\right)+\frac{\partial}{\partial y}\left(\frac{v_r}{2}\left(\frac{\partial(\rho h)}{\partial y}\right)\right) \quad (19)$$

The fluid velocity profile on the x-axis direction $u_f$:

$$\frac{\partial^2}{\partial z^2}\left(u_f(x,y)\right)=\frac{1}{\eta}\frac{\partial p}{\partial x}$$

$$\frac{\partial}{\partial z}\left(\eta\cdot u_f(x,y)\right)=\frac{\partial p}{\partial x}$$

$$\frac{\partial}{\partial z}\left(\eta\cdot\frac{\partial u_f}{\partial z}\right)=\frac{\partial p}{\partial x}$$

$$\frac{\partial u_f}{\partial z}=\frac{z}{\eta}\cdot\frac{\partial p}{\partial x}+\frac{1}{\eta}\cdot C_3$$

$$u_f=\frac{z^2}{2\cdot\eta}\cdot\frac{\partial p}{\partial x}+\frac{1}{\eta}\cdot C_1\cdot z+C_2 \quad (20)$$

And consequently, the fluid velocity profile on the y-axis direction $v_f$:

$$\frac{\partial^2}{\partial z^2}\big(v_f(x,y)\big) = \frac{1}{\eta}\frac{\partial p}{\partial y}$$

$$\frac{\partial}{\partial z}\big(\eta \cdot \ v_f(x,y)\big) = \frac{\partial p}{\partial y}$$

$$\frac{\partial}{\partial z}\left(\eta \cdot \frac{\partial v_f}{\partial z}\right) = \frac{\partial p}{\partial y}$$

$$\frac{\partial v_f}{\partial z} = \frac{z}{\eta}\cdot\frac{\partial p}{\partial y} + \frac{1}{\eta}\cdot C_1$$

$$v_f = \frac{z^2}{2\cdot\eta}\cdot\frac{\partial p}{\partial x} + \frac{1}{\eta}\cdot C_3 \cdot z + C_4 \qquad (21)$$

To adjust the velocity profiles to the study case, the following boundary conditions are imposed:

$$h = h_0 + \Delta h \qquad (22)$$

This way,

$$u_f(x,y,0) = -r\cdot\omega\cdot\sin\theta \qquad (23)$$

$$u_f(x,y,h) = 0 \qquad (24)$$

Finally, the equations system is solved:

$$u_f(x,y,0) = C_2 \rightarrow C_2 = -r\cdot\omega\cdot\sin\theta \qquad (25)$$

$$u_f(x,y,h) = \frac{h^2}{2\cdot\eta}\cdot\frac{\partial p}{\partial x} + \frac{1}{\eta}\cdot C_1\cdot h + (-r\cdot\omega\cdot\sin\theta) = 0 \qquad (26)$$

$$C_1 = \left(-\frac{h}{2}\cdot\frac{\partial p}{\partial x} + \frac{\eta\cdot\ r\cdot\omega\cdot\sin\theta}{h}\right) \qquad (27)$$

The same procedure is followed for the other direction:

$$v_f(x,y,0) = r \cdot \omega \cdot \cos\theta \tag{28}$$

$$v_f(x,y,0) = C_4 \rightarrow C_4 = r \cdot \omega \cdot \cos\theta \tag{29}$$

$$v_f(x,y,h) = \frac{h^2}{2 \cdot \eta} \cdot \frac{\partial p}{\partial y} + \frac{1}{\eta} \cdot C_3 \cdot h + (r \cdot \omega \cdot \cos\theta) = 0 \tag{30}$$

$$v_f(x,y,h) = 0 \tag{31}$$

$$C_3 = \left(-\frac{h}{2} \cdot \frac{\partial p}{\partial y} - \frac{\eta \cdot r \cdot \omega \cdot \cos\theta}{h}\right) \tag{32}$$

The expression for $u_f(x,y,z)$ is:

$$u_f(x,y,z) = \frac{z^2}{2 \cdot \eta} \cdot \frac{\partial p}{\partial x} + \frac{1}{\eta} \cdot \left(-\frac{h}{2} \cdot \frac{\partial p}{\partial x} + \frac{\eta \cdot r \cdot \omega \cdot \sin\theta}{h}\right) \cdot z - r \cdot \omega \cdot \sin\theta \tag{33}$$

The expression for $v_f(x,y,z)$ is:

$$v_f(x,y,z) = \frac{z^2}{2 \cdot \eta} \cdot \frac{\partial p}{\partial y} + \frac{1}{\eta} \cdot \left(-\frac{h}{2} \cdot \frac{\partial p}{\partial y} - \frac{\eta \cdot r \cdot \omega \cdot \cos\theta}{h}\right) \cdot z + r \cdot \omega \cdot \cos\theta \tag{34}$$

The expressions from both velocity fields are parabolic. The velocity in each direction is the one showed in *Figure 8*.

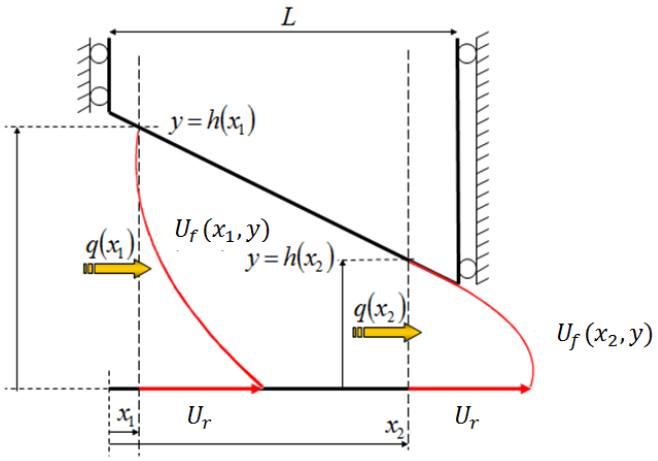


*Figure 8. Velocity profile from solving the one dimension Reynolds equation.*

Finally, combining the velocity profile in each direction:

$$U_f(x,y,z) = \sqrt{u_f(x,y,z)^2 + v_f(x,y,z)^2} \tag{35}$$

It will be useful in advanced models when it is important to take into account the viscous heating in order to predict the fluid temperature distribution.

It is possible to apply a more accurate gap definition but the problem turns out really complex when the gap morphology is exactly modelled from the deformations from the pad and the collar. In addition, for a 3D geometry, a proper velocity profile should take into account the side leakage. It should also include the transition laminar-to-turbulent flow of the fluid film.

*Figure 9* shows the velocity field obtained taking into account complex gap geometry due to pad and collar elastic deformations.

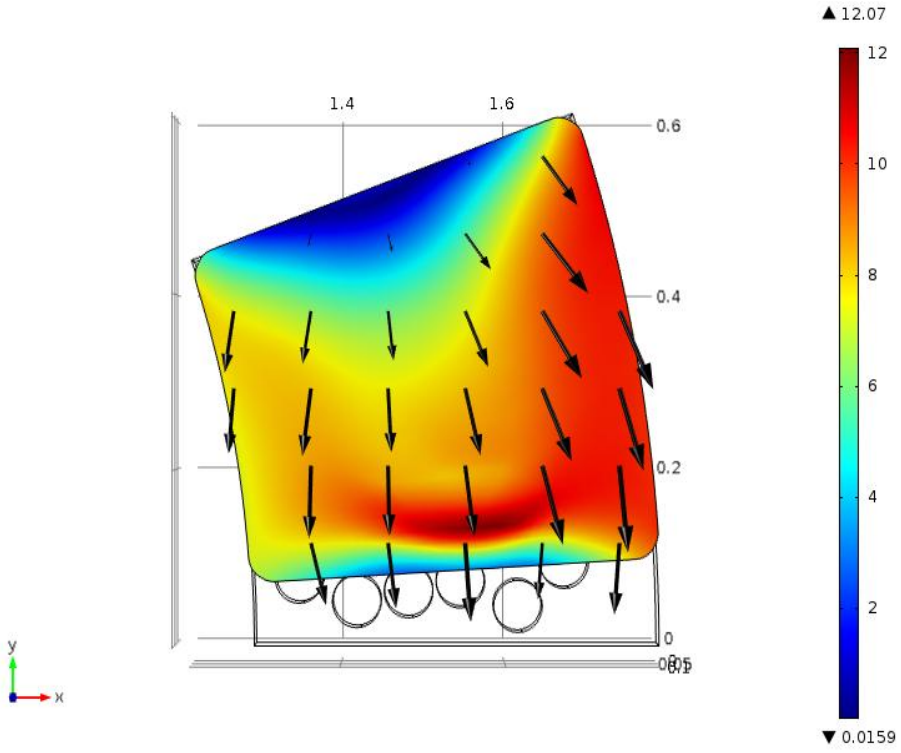


*Figure 9. Velocity field for z = h/2 obtained from solving the Reynolds equation with a variable accurately defined gap profile.*

### 4.1.5 Negative Pressures: Cavitation

The geometry of the fluid layer plays a relevant role on the pressure and velocity distribution. The morphology of the gap, apart from defining the pressure distribution is responsible of the sign of this pressure. Bear in mind that these pressures are extremely high and a dozen of mega Pascal difference on few centimetres affects heavily pad and collar surfaces.

When the resulting gap geometry is absolutely convergent, without any divergent stretch, the pressure achieved is totally positive; the sign of the pressure distribution relies on the gap specific shape. Moreover, when the gap becomes divergent, negative pressures appear on the tract.

Under certain conditions, the gap shows a convergent-divergent profile *(Figure 10)*, giving this way a complex pressure distribution.

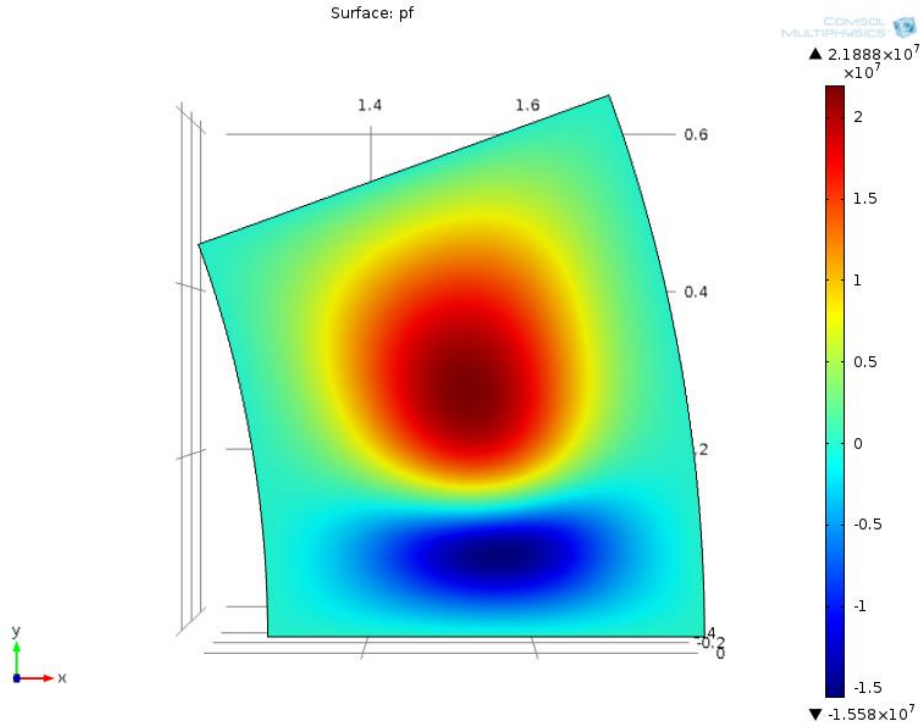


*Figure 10. Pressure distribution from a convergent-divergent gap resultant profile.*

The most part of the researchers who worked with the Reynolds equation agree that the gap geometry is the key factor to deal with. Somerfeldt [38] pointed out this phenomenon studying the following gap geometry profile *(Figure 11)*.

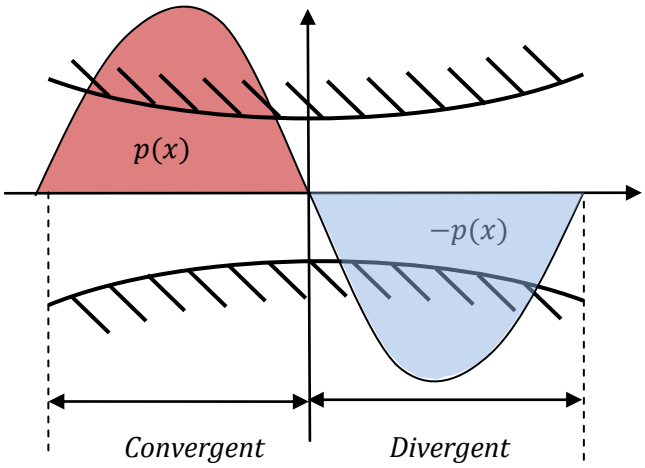


*Figure 11. Sommerfeldt pressure distribution.*

A high negative pressure region implies cavitation. Cavitation is the formation and then immediate implosion of cavities in a liquid – i.e. small liquid-free zone ("bubbles") – that

are the consequence of forces acting upon the liquid [39]. Cavitation is a worrying phenomenon when designing any hydrodynamic device with fast motion pieces. It generally limits the operating conditions. Cavitation decreases the efficiency of the thrust bearing and in some cases can produce the failure of it.

Some mathematical procedures are commonly followed to overcome the problems associated with the negative pressures. A simple one consists of neglecting the negative pressures. Just take into account the positive pressure and assume that the pressure is zero on the negative region due to the cavitation phenomenon [38] means that:

$$p' = max\ (p, 0) \qquad (36)$$

It is mathematically represented with a penalty term in the Reynolds equation. This is an inaccurate simple procedure. Other approaches consist in applying a balance on the cavitation region based on the continuity equation *(Eq. 37),* being $A_A$ and $A_B$ the section of the gap at the beginning and the ending of the negative pressures region.

$$v_{f_A} \cdot A_A = v_{f_B} \cdot A_B \qquad (37)$$

Finally, it is decided to define the pressure as a piecewise function similar to *Eq. 36*( 36 ).

$$p' = p \cdot H_e \qquad (38)$$

$$H_e = 1\ (p > e)$$
$$H_e = 0\ (p < e)$$

The corrected pressure $p'$ obtained is shown for 2D and 3D models in *Figure 12* and *Figure 13* respectively. To ensure the continuity of the pressure a 5th degree function has been defined on the transition. The boundary value $e$ is responsible to define where is the transition must be. This value can be modified in order to match the results with some experimental measurements. The pressure applied in the other models is also multiplied for the piecewise function $H_e$ *(Eq. 38)*.

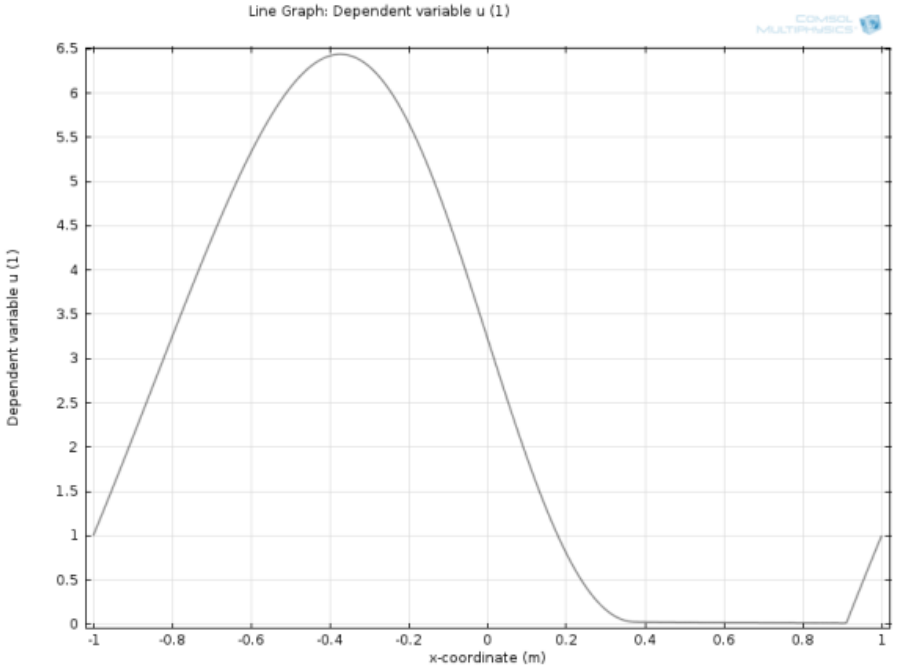


*Figure 12. Cavitation is taking into account a defining a piecewise function.*

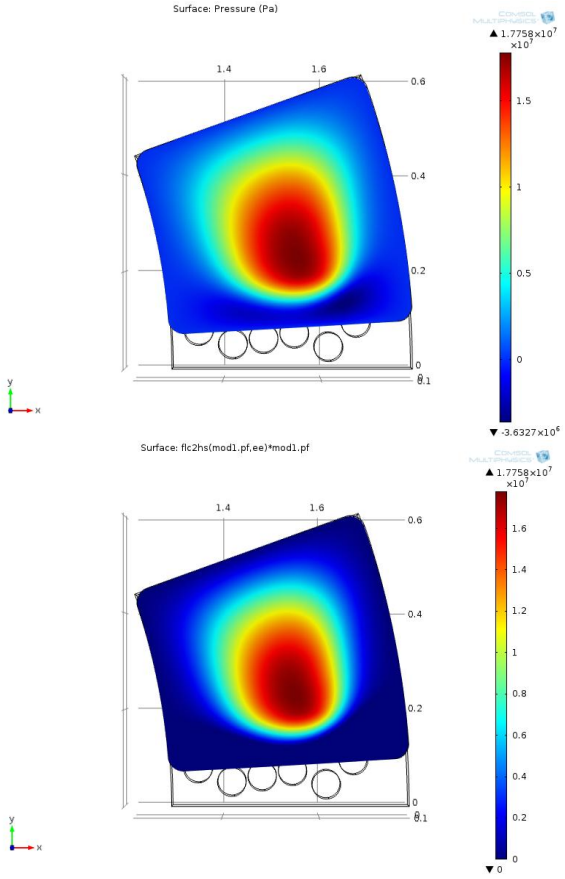


*Figure 13. Pressure distribution corrected when taking into account the cavitation applying the piecewise function He.*

## 4.2 Solid Mechanics

After well-defining the pressure distribution, the next step by order of importance is to include the counteraction of the solids where the pressure is applied, i.e. on the pad and the collar. As Ettles stated, there is a size effect when working with thrust bearings, requiring increasing attention to the control of deformation as the size is increased [19]. So the model is implemented as a solid mechanic allowing its deformation *(Figure 14)*. The proprieties of the materials compounding the assembly are also input.

The FEM model outputs for this particular model are these four variables:

1) Pressure of the lubricant film $p$
2) Deformation in x-direction $u$
3) Deformation in y-direction $v$
4) Deformation in z-direction $w$

Therefore, four equations are needed to compute the solution of the model:

1.) Reynolds equation
2.) Pressure distribution adjusted to the external load $Wext$
3.) Isotropic Elastic Material Behaviour Expression
4.) Gap Geometry

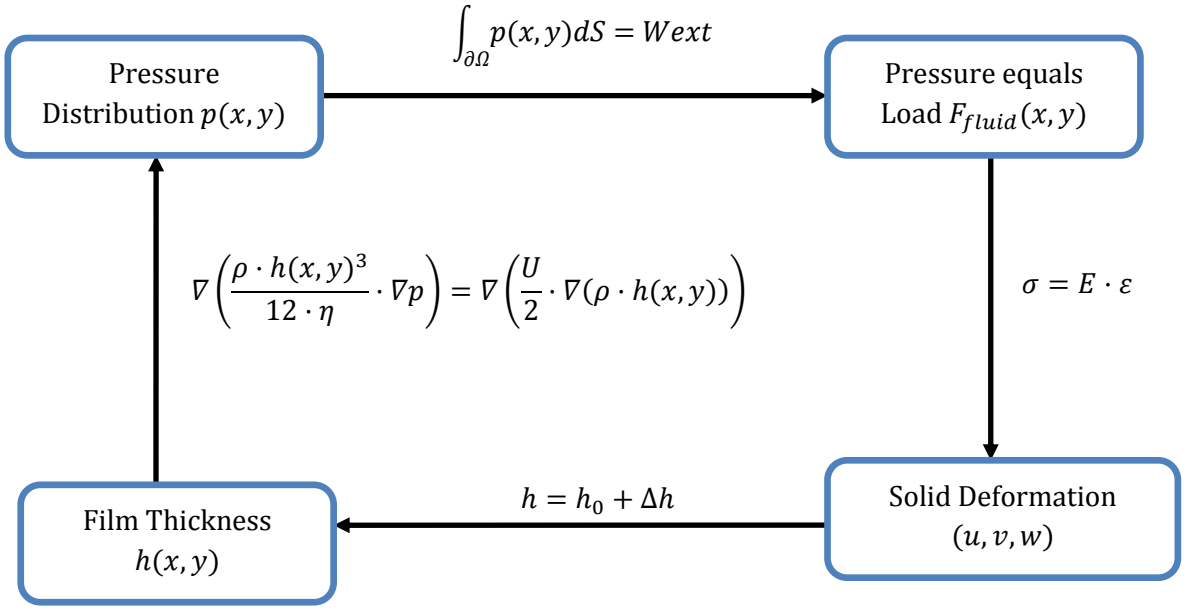


*Figure 14. Solver scheme coupling a defined pressure distribution and mechanical deflection suffered for both pad and collar.*

After an iterative procedure the results converge in a solution. Obtaining this way the deformation suffered for the solids and the pressure distribution on the gap.

### 4.2.1 Lineal Elastic Material Model

In order to implement the deformation suffered by pad and collar, an isotropic lineal elastic material has been chosen. Every node from the mesh follows the Hooke's Equation obtaining this way the components of the displacement field $u, v, w$.

The main handicap of thrust prediction models is the whole system strong linkage. In this case, the deflection suffered on surfaces due to the pressure applied modifies at the same time the gap geometry varying also the pressure exerted. Hence it is a matter of iterations. The solving procedure has to be repeated until the results converge into a defined tolerance (the tolerance is adjusted to $10^{-6}$ in the whole study).

A tough part is to define a proper gap geometry taking into account the most important phenomena.

As seen in *Figure 15*, this study has taken into account the tilting balance and both elastic and thermal deformations from the pad and the collar. Both materials from pad and collar are considered lineal elastic.

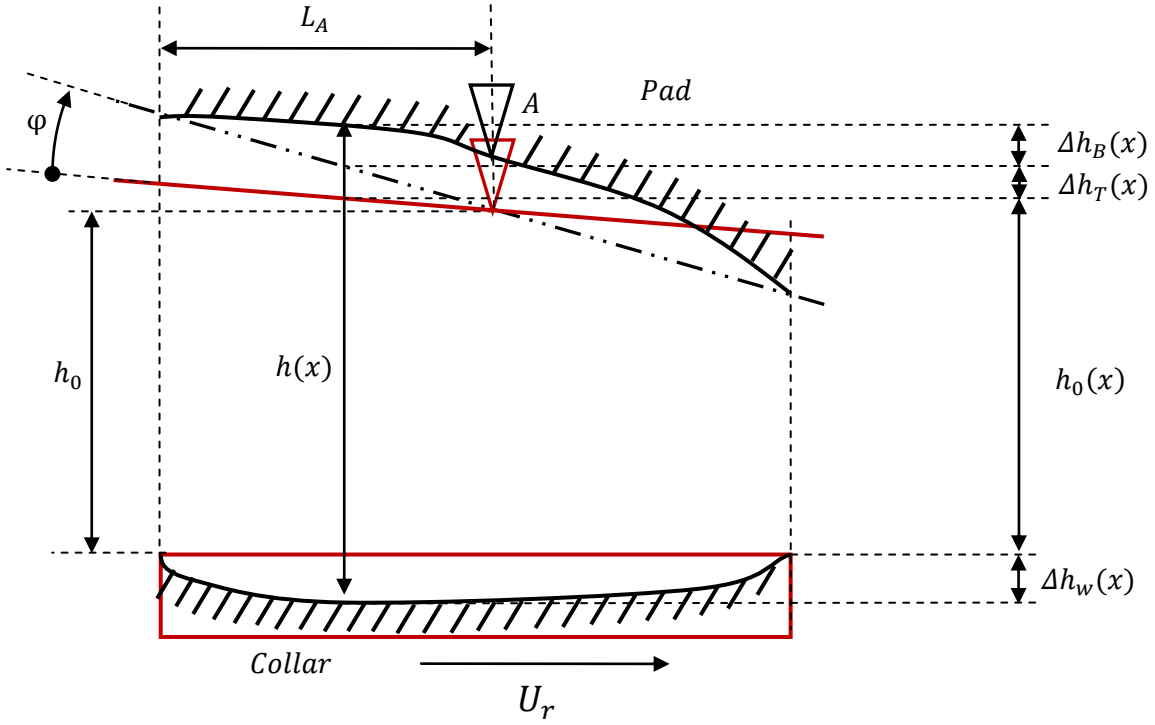


*Figure 15. Pad and collar deformation scheme.*

$\varphi$ *Angle between the initial position and the tilted one*
$h_0$ *Intial Gap Inclination*
$\Delta h_T$ *Tilt of the Pad*
$\Delta h_B$ *Deformation of the Channel Base*
$\Delta h_w$ *Deformation of the Solid Wall*

$h(x)$ Final Gap Geometry:

$$h_0(x) = h_0 + (L_A - x) \cdot \tan\varphi \quad (39)$$

$$h(x) = h_0 + \Delta h_w + \Delta h_B + \Delta h_T \quad (40)$$

At the beginning, the deformation was studied as a tilting pad thrust bearing (TPTB); the pad tilts $\Delta h_T$ over a defined pivot point. Although the tilting problem is finally solved without considering a defined pivot point, the gap general expression *(Eq. 40)* remains the same in the models.

### 4.2.2 Freedom Degrees and Constraints

The pressure applied on the upper surface of the pad is obtained from solving the 2-dimensions Reynolds Equation. The inputs for that expression are the density $\rho$ and viscosity $\eta$ of the fluid, the velocity field of the collar $u_r$ , $v_r$ , $w_r$ and the gap geometry $h(x, y)$.

Up to this point, the fluid properties are considered constant. Thermal effects are not taken into account yet. The boundary condition of zero pressure at the edges is an input. The pressures applied on pad and collar surfaces have also been assumed equal.

It is not an easy task to provide the model with the tilting capacity. It has not been found in many of the research papers available. The pad deflection has been generally approached by finite difference methods. The biharmonic thin plate equation does not allow inputting this propriety without violating the thin plate assumptions. It is right that the tilting variation is minimal, however, as is has been seen *(Figure 3)*; the pressure can be extremely influenced by the pad inclination. The best approach is found by Brown whose model solved the pad deflection using finite element methods [26].

As Boudry reported [40], a single pivot support yields a high peak pressure which should be avoided by supporting the pad on a large number of points to obtain an optimum pressure profile i.e. instead of point or line support, use of ring/disc support is preferable. Spring-supported thrust bearings are one kind of the called multi-support systems and allow the possibility of a bidirectional rotation for the runner.

### 4.2.3 Tilting over a Defined Pivot Point

There are two ways of facing this problem: the first one consists in modelling the pad when it is already tilted; applying on the model the final running conditions. The pressure applied on the model is already defined with the real inclination under the working conditions. In this method the real pad inclination is required and, unfortunately this data is difficult to measure and even thus, the tilting angle is far to be a constant value. Many models conclude with a pad inclination sweep [33]. This was also done in the present

study, see *Figure 3*. Although it helps to understand the relevance of the tilting phenomenon it has not any practical application.

The second way consist in inputting the initial conditions that make the model tilt in order to fulfil the mechanical equilibrium conditions. The problem on this way is to take into account the wide range of factors that defined the pad tilting angle. In the best case, the inclination obtained must match with the operating one.

Both ways have been considered in this work however lately it has been seen that the first one is not physically performable, for the application of the study. Apparently, when considering the pad deformation and thermal expansion the problem does not deal with flat surfaces anymore so it becomes very difficult to define the inclination.

The first method, with a fixed inclination, defines the gap as a plane (3D model) or a line (2D model). This is illustrated in *Figure 16*.

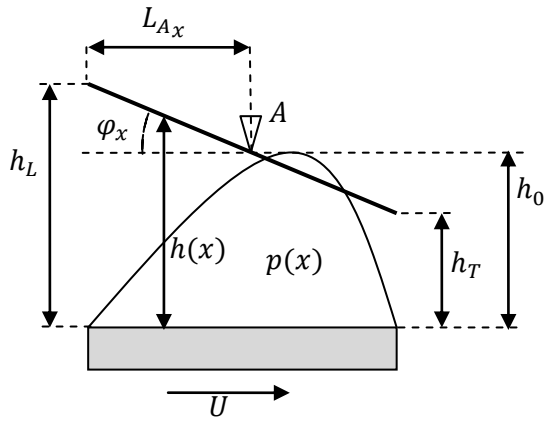


2D Model:

$$h(x) = h_0 + k_x \cdot x \qquad (41)$$
$$k_x = tan\ \varphi_x$$

3D Model:

$$h(x, y) = h_0 + k_x \cdot x + k_y \cdot y \qquad (42)$$
$$k_x = \tan \varphi_x$$
$$k_y = \tan \varphi_y$$

*Figure 16. Tilting scheme defined on a 2D model.*

In the second method, much more complex, the inclination angle is not an input. So the pad inclination is deduced from ensuring that the sum of moments on the upper surface must be null *(Eq. 43)*.

$$\int_0^L p(x) \cdot (L_{A_x} - x) dx = 0 \qquad (43)$$

That can easily be applied on a 3D model considering both axial directions and defining the pivot point using two coordinates $(L_{A_x}, L_{A_y})$.

Xiaojing Wang [24] proofed that different spring patterns and their characteristics can alter significantly the behaviour of the pad. Actually, the springs are only involved when tilting is included. The first method, where the pad inclination is directly an input based on empirical measurements, there is no point in including the springs in the model.

The spring's pattern behaviour has been simplified to only two phenomena *(Figure 17)*. One is the uniform compression of the springs, the pad translation $\delta$ along the $z$ direction, in order to compensate the external load applied. The other phenomenon is the pad tilt, countered by a resistive moment $M_{springs}$. The pivot point has been located on the

equivalent position of the spring mattress pattern $(L_{A_x}, L_{A_y})$. The location of the resultant point is obtained via a moment balance on the pad surface *(Eq. 50* and *Eq. 51).*

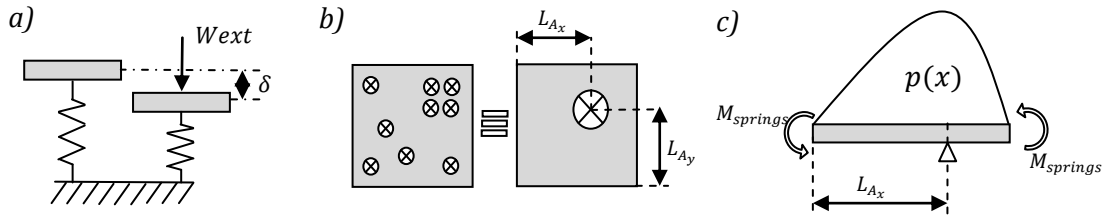


*Figure 17. Characterization of a spring-supported trust bearing. a) Uniform sagging when applying the load on the pad. b) Assimilation of a springs patter on unique spring on a concrete point. c) Diagram of the pad and the considered loads.*

Assuming this spring's behaviour, the following constraint *(Eq. 44)* must be included to ensure the balance of the model:

$$\int_0^L p(x) \cdot (L_A - x)dx - M_{springs} = 0 \qquad (44)$$

The uniform pad translation δ , needed to counter the external load Wext applied, is taken into account to define the initial gap between pad and collar in the Reynolds equation $h_0$.

Despite all the considerations taken into account, this model is closer to a tilted-pad thrust bearing than to a spring-supported one. The model is tilting over one point. Due to the difficult convergence found when testing this method, it was decided to model the springs in a more realistic sense.

### 4.2.4 Tilting without a Defined Pivot Point

The point in this method is to integrate the characteristics of a spring mattress in a solid mechanics domain with linear elastic cylinders representing the spring mattress. The tricky stage in this approach is to adjust the material proprieties. Basically, it means that the Young's modulus $E$ needs to be matched with the elastic constant of a spring $k$. According to Hooke's Law linear elastic materials displays the following property;

$$\sigma = E \cdot \varepsilon \qquad (45)$$

And linear elastic springs obey the following constitutive equation:

$$F = k \cdot \delta \qquad (46)$$

Adjusting the material proprieties, a narrow prismatic brick has been attached to the model. The results are shown in *Figure 18*¡**Error! No se encuentra el origen de la referencia.**.

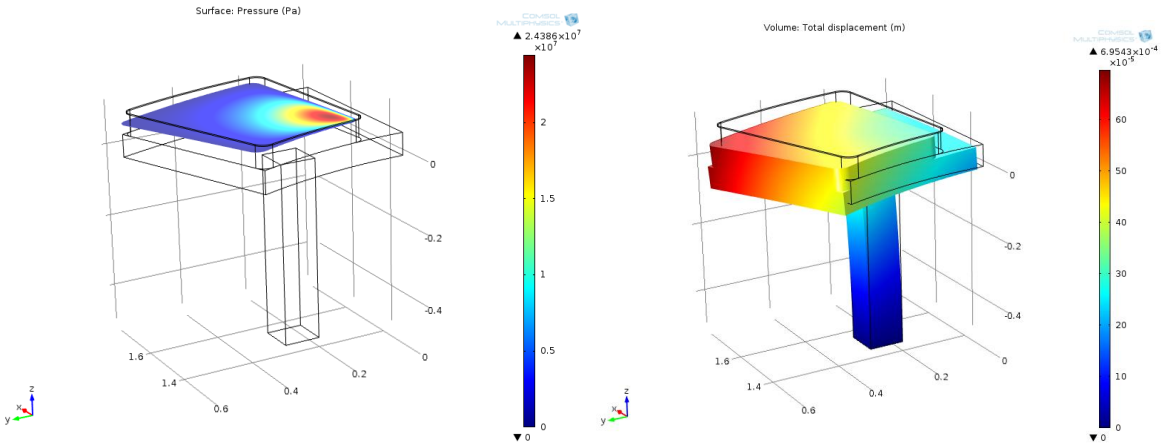


*Figure 18. Pressure distribution and displacement obtained from simulating the spring-supported behaviour as a lineal elastic solid brick in a defined position.*

Despite it is an inaccurate simulation using inaccurate parameters, it is clear that the pad is tilting in the proper direction.

The material proprieties and the dimensions of the prismatic brick must be adjusted in order to limit the randomness of the results. In addition, that way of overcoming the tilting problem seems to behave closer to a spring mattress support.

There are many configurations available:

a) A unique volume with the same area as the pad lower surface.
b) A unique volume that behaves as the resultant spring deduced from the springs pattern.
c) Implement every spring independently and model each spring with its respective position with a defined geometry.

Even if there is not a fixed pivot point, the location of the volumes and their direction plays an important role *(Figure 19)*.

In the case a) the area of the volume is already defined so a pivot point cannot be input. Even though, the height of the surface, which represents the effective spring length, will be determining.

The spring constant $k$ is related with the Young Modulus $E_s$ by the following expression:

$$k_s = \frac{E_s \cdot A_s}{d_s} \qquad (47)$$

The Young Modulus $E_s$ can be deduced from defined geometry $\frac{A_s}{d_s}$. Where the strain $\varepsilon$ and the deformation $\delta$ are related according to:

$$\varepsilon = \frac{\delta}{L} \tag{48}$$

For a spring mattress, the equivalent spring constant $k_E$ can be easily achieved by summing the spring constants.

$$k_{s_E} = \sum_{i=1}^{n_s} k_{s_i} \tag{49}$$

The equivalent pivot point location $(L_{A_x}, L_{A_y})$ is obtained from a moment balance calculation where the spring constant $k_{s_i}$ is taken as the weight and the distance from each spring $i$ to a common point is $(L_{s_{x_i}}, L_{s_{y_i}})$:

$$L_{A_x} = \frac{\sum_{i=1}^{n_s} k_{s_i} \cdot L_{s_{x_i}}}{\sum_{i=1}^{n_s} k_{s_i}} \tag{50}$$

$$L_{A_y} = \frac{\sum_{i=1}^{n_s} k_{s_i} \cdot L_{s_{y_i}}}{\sum_{i=1}^{n_s} k_{s_i}} \tag{51}$$

There is still the inconvenience of defining a proper $\frac{A_s}{d_s}$ parameter.

The results obtained showed that the bigger is $d_s$, the higher deformation is suffered. However, the pressure applied on the pad does not vary significantly with L variations.

As it was expected, the position of the volume representing the spring's equivalent is too relevant when obtaining a tilted inclination. It is shown in *Figure 19*.

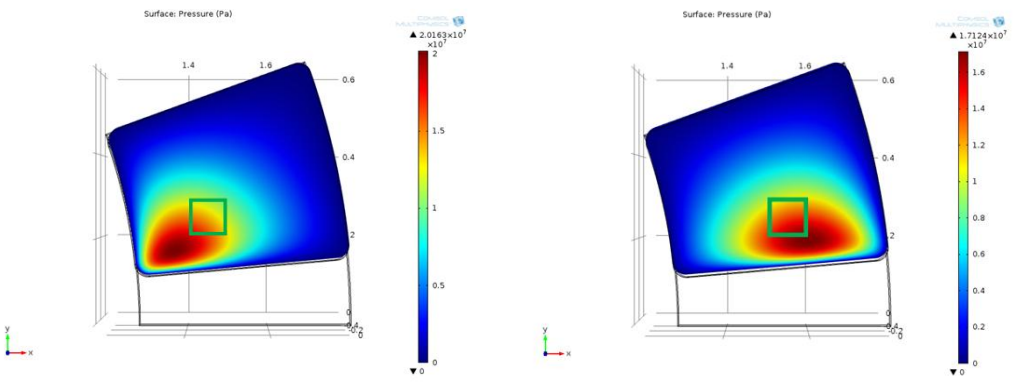


*Figure 19. Pressure distributions achieved changing the brick position.*

From the literature available, it is known that the pivot point is offset between the 50% and 65% of the pad extent from the leading edge [26].

Due to the excessive relevance of the location of the brick performing as the mattress of springs, it is decided to match its base with all the pad extension (option b).

As Wang stated [24], a uniform distribution of springs in the full extent of the pad results a bad performance and removing the springs in the inlet zone, especially those at the mean radius and its vicinity, can be beneficial to the oil wedge formation and thus to the pad behaviour. The pad tilts randomly on both ways as it has been seen on the simulations. In addition, the operating conditions range becomes really small to ensure the gap convergence. As a result, a negative pressure area shows up easily.

Instead of varying the spring's distribution or using different springs for each region, an equivalent method was followed fifty years ago when designing the thrust bearing under study. This method consists in removing material from the pad to locate the highest lubricant pressure on a smaller offset surface *(Figure 20)*. The mass centre is also displaced; although it plays a small role compared with the operating pressure. These bearings are called step thrust bearings.

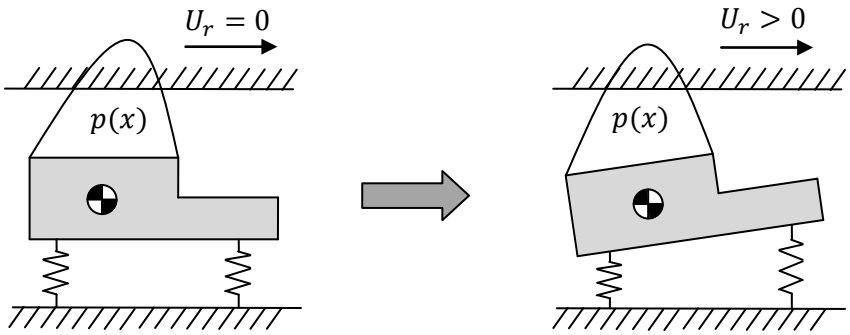


*Figure 20. Spring-supported step thrust bearing behavior.*

This way, using a constant Young's Modulus for the material that represents the spring's mattress, the pad tilts to avoid any unstable position. Even if the pad is now allowed to tilt, the results are still far from the correct ones. The model results are compared with empirical studies in order to adjust the material parameters. Although this method is viable, it is difficult to adjust so it is decided to proceed with last option.

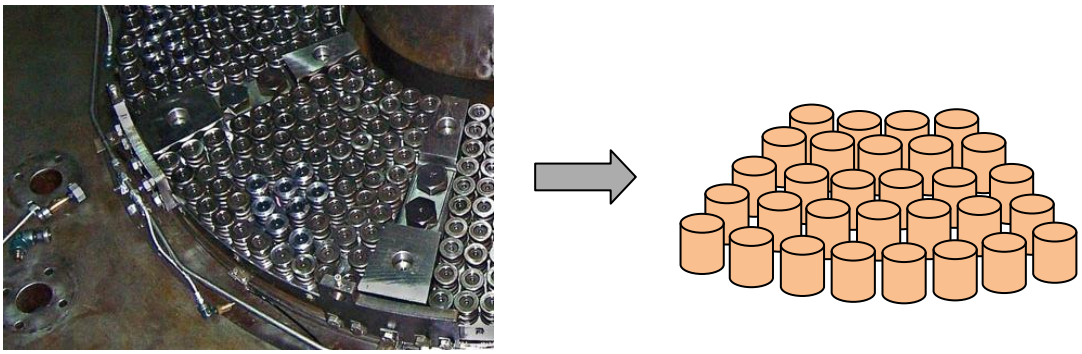

*Figure 21. Option c) Implement every spring independently and model each spring with its respective position with a defined geometry.*

Finally, it is decided to copy the real spring mattress morphology (option c), see *Figure 21*. Cylindrical blocks of material were used to model the springs. Every cylinder represents a single spring. It has been modelled using the height of the already compressed spring (effective height) and an approximate diameter value. The Young modulus of the material representing the springs have been obtained by the formula which relates $k$ and $E$ using the sum of the areas of the cylinders and their height. Unfortunately, it was imprecise so and adaption to the experimental results was needed. This method for simulating the springs increases heavily the modelling and meshing task. It also requires much more time to solve.

### 4.2.5 External Load

Thrust bearings are useful when it comes to carry huge axial loads, commonly the shaft from a hydroelectric turbine.

This load is applied to the lubricant film generating high pressures that are transmitted equally to pad and runner surfaces. The external load is a common input in thrust bearings models. The load to carry is easy to estimate and it is a useful input in order to predict the effects of applying different loads without risking the real turbine.

The equation below ensures that the fluid pressure into the gap equals the external load applied:

$$\int_{\partial\Omega} pdS = F_{fluid} = W_{ext} \qquad (52)$$

A comparison has been carried out between adding a defined external load or not. To test the goodness of the new constraint included *(Eq. 52)*, the pressure distribution has been integrated over the entire surface where is applied to get the load carrying capacity. It obviously matches with the load carrying capacity.

Taking into account the cavitation phenomenon, the pressure in the expression above is the one defined as a piecewise function where the pressures are null in the negative pressure regions.

This pressure achieved is also applied on the runner surface. This assumption is a tricky one because the runner is rotating at the shaft's angular velocity. Although it is a high angular velocity, a non constant pressure is applied on the collar surface. The pressure applied must be considered, under stationary conditions, an average between the pressure applied on the pad and the one applied to the non pad area (groove and pad step), see *Figure 22*.

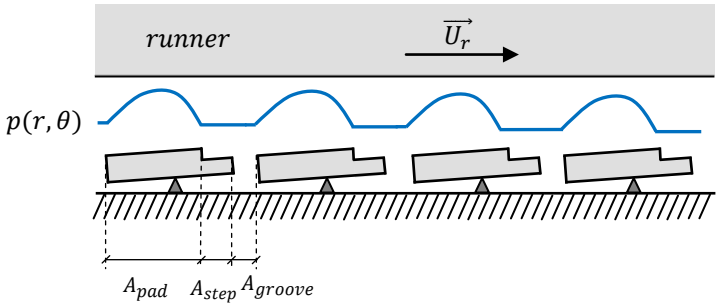


*Figure 22. Pressure applied on the runner due to pressure generated on the pads.*

A factor conditioning the pressure exerted $k_c$ can be applied in defined by the pad area $A_{pad}$ , the groove area $A_{groove}$ and the step area $A_{step}$.

$$k_c = \frac{A_{pad}}{A_{step} + A_{groove}} \qquad (53)$$

The goodness of this approximation is difficult to proof. This phenomenon is partially responsible of the vibrations suffered in the thrust bearing when working under normal conditions. This load fluctuation has been studied by Estorteig [25]. This effect is not included on the present work.

It is difficult to predict whether the case with or without applied loading will be more liable to fail. When the pressure is applied and when it is not, both can be dangerous under certain conditions. In this study the full load has been considered, however a factor can be easily input reducing the pressure applied.

### 4.2.6 Pad and Collar Deformation

The most part of the papers point out the importance of having into account the pad and collar deformation in order to achieve correct results. When working with thrust bearings, where a small inclination variation involves a huge difference on the results, it is unacceptable to consider the surfaces of the pad and the collar as rigid solids.

The pad deformation is solved by coupling the surface deformation with the gap geometry. The iteration followed inputs the solid wall deformation suffered on the solid mechanic element.

A common method to consider the collar deformation is to create an equivalent Young's modulus and Poisson's ratio [41]. That approach consists in the estimation of an equivalent Young modulus and Possion coefficient from the pad and runner material [42]. In this way, it is estimated that the pad and the collar suffer the same deformation:

$$E_{eq} = \frac{E_p \cdot E_r}{E_p + E_r} \quad (54)$$

$$\upsilon_{eq} = \frac{\upsilon_p \cdot E_r + \upsilon_r \cdot E_p}{E_p + E_r} \quad (55)$$

Some revised expressions have been published [43]:

$$E_{eq} = \frac{E_p^2 \cdot E_r \cdot (1+\upsilon_r)^2 + E_r^2 \cdot E_p \cdot \left(1+\upsilon_p\right)^2}{\left[E_p \cdot (1+\upsilon_r) + E_r \cdot \left(1+\upsilon_p\right)\right]^2} \quad (56)$$

$$\upsilon_{eq} = \frac{E_p \cdot \upsilon_r \cdot (1+\upsilon_r) + E_r \cdot \upsilon_p \cdot \left(1+\upsilon_p\right)}{E_p \cdot (1+\upsilon_r) + E_r \cdot \left(1+\upsilon_p\right)} \quad (57)$$

When it comes to consider the pad and collar deformation, adding the spring's pattern to the model as a linear elastic material involves some drawbacks. The deformation of the solid wall (pad upper surface) it is included in the gap definition as it was explained before. That deformation consists of the pad inclination and the pad surface deformation. In this case, the collar deformation cannot be assumed the same as the pad deformation. The collar cannot vary its inclination and in addition, the collar is a motion piece therefore the deformation will be different. So the displacement field of the collar must be achieved by another way.

Although most of the papers skip this step arguing that it is a waste of time and computational resources, the present study indicates the necessity modelling also the collar. That doubles the complexity of the complexity of the algorithm since it doubles the number of nodes. However, adding a solid model for the collar allows inputting a proper material for the collar without assuming an equivalent Young modulus. It is also useful to check the role of the elements joining the runner and the shaft (something desired by the company in charge of the turbine).

To simplify the calculation procedure, the pressure on pad and collar are assumed equal. Which means that the pressure distribution obtained from solving the Reynolds Equation on the pad is applied on the collar too. This way, the Reynolds Equation only needs to be solved once. Then, the deformation suffered on the collar is also included to the gap variable geometry in the pressure calculation.

Finally, with cylindrical blocks behaving as the spring mattress and both pad and collar deformations taken into account, the tilting and the deformation phenomena are considered.

$$h(x,y) = \underbrace{h_0}_{\text{Initial Gap Geometry}} + \underbrace{\Delta h_B}_{\text{Collar Deformation}} + \underbrace{\Delta h_W + \Delta h_T}_{\text{Pad Deformation}} \quad (58)$$

As it is seen, the initial gap geometry $h_0$ plays a weak role in the final gap definition but it is essential to enter a good initial guess for the iterative solution process to converge.

## 4.3 Thermal Effects

The importance of considering thermal effects when simulating large tilting pads is confirmed in the most part of the articles published. Taking thermal effects into account means considering heat transfer, thermal expansion and link some material properties to the resultant temperature distribution. According to the literature review, the density and the viscosity of the fluid must be considered as dependent of the temperature. A third geometry is modelled performing as the fluid film located between the pad and the collar.

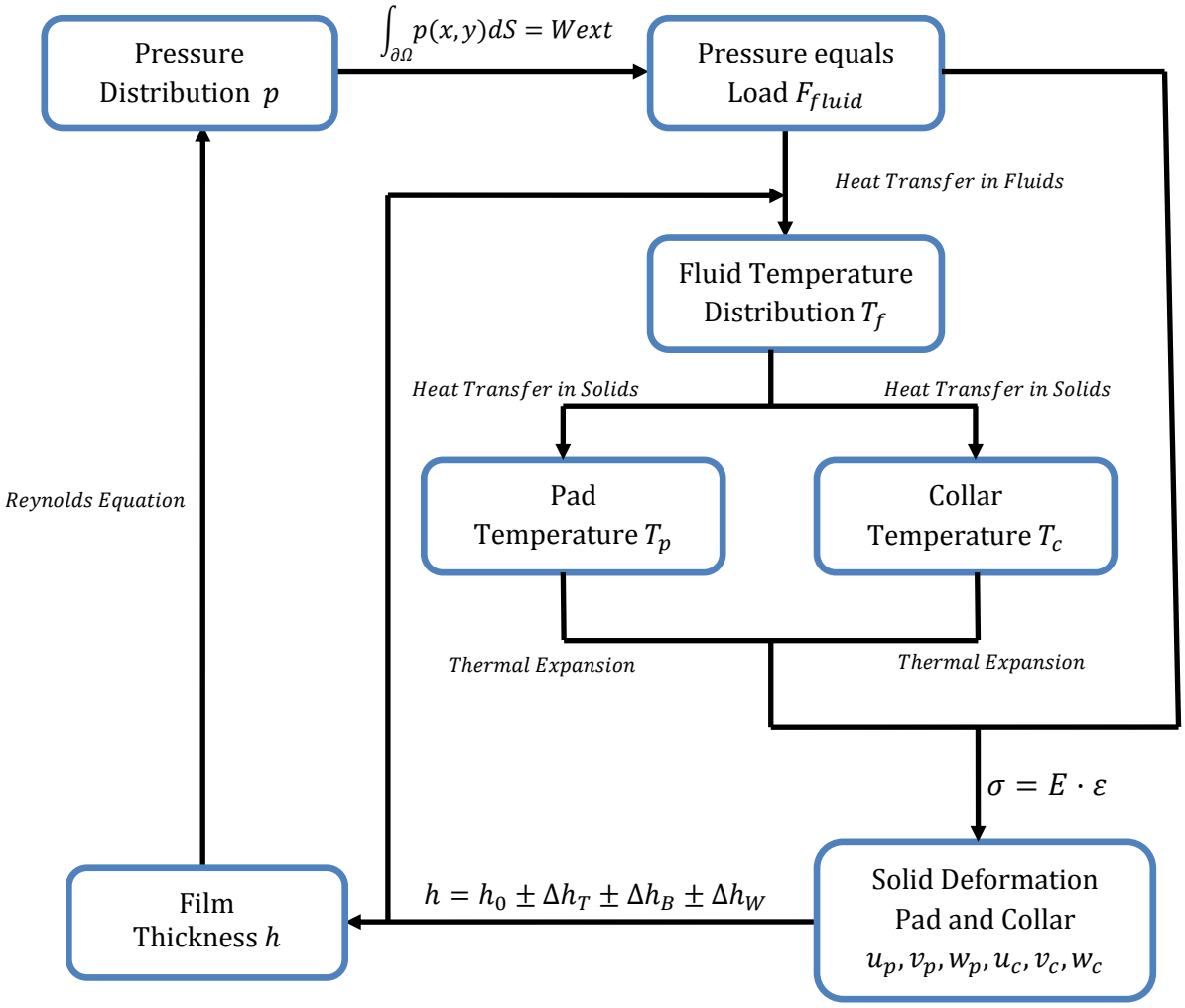


*Figure 23. Equation system linkage resultant from considering the thermal effect to the model.*

In order to take thermal effects into account; two different physics must be coupled. The temperature distributions of the pad and collar surfaces from the fluid model are the boundary conditions to solve the heat transfer in solids equation in the pad and the collar models.

This gives the temperature distribution in both pad and collar. This solution procedure requires boundary conditions for the solid-fluid boundaries, which will be defined later. Having the temperature distribution in the entire assembly makes possible to calculate the

thermal expansion and to consider the variation of the material properties due to temperature raise.

The complexity of the simulation has been increased considerably, giving the equation system depicted in *Figure 23*.

The whole system will be iterated until the difference between consecutive results is small enough to consider that it has already converged. The physics influencing convergence characteristics the most is the lubricant shell physics, in which Reynolds equation is the governing equation.

### 4.3.1 Temperature Distribution of the Fluid Film

There are many studies focused on determining the operating temperatures of thrust bearings. It is a tough problem due to the amount of phenomena involved. There are two ways of considering this issue; by hydrodynamics or by thermodynamics. The first one consists in studying the fluid as a volume of its won, with boundary conditions formulated from the flow rate at the leading and trailing edge and the side leakage. It also requires going deeper into the laminar-turbulent proprieties. From the literature review it is concluded that it is really difficult to define these parameters, since they are both difficult to measure and to predict. Tieu (for example) tried to approach the problem this way and came across many uncertainties [43]. For these reasons the fluid temperature distribution is considered through a heat transfer balance.

It is difficult to study a specific part of a thrust bearing such as the fluid layer because it is affected for the pad and runner heat transfer with their cooling tubes. Also the groove between pads has many articles just for itself [10] [45] [9]. The pad is immersed in an oil bath which is also affects the viscous heating.

The lubricant film is located in between the pad and the collar. Due to the fact that the slip phenomenon on the fluid-solid interface is not considered, the fluid has exactly the same velocity as the wall at the contact surface. The fluid is moving between these two walls with its own velocity field.

In mot papers dealing with this subject, the temperature in the fluid is not assumed to vary across the height film. In this thesis, the $z$ direction is taken into account when solving the energy equation *(Eq. 59)*. This means that the fluid temperature may vary also with the height of the film.

Some inaccuracies are introduced modelling the fluid layer. As it has been seen, both surfaces (pad and collar) suffer deformations so the gap between them is not flat anymore. It is difficult to predict the fluid velocity field, even more considering the new gap geometry. As first step, approaching this problem, both surfaces are assumed to be flat. The average deformations of the pad and the collar were then considered to define the distance between the two flat surfaces, i.e., the fluid film thickness. This connection

between the fluid geometry and the deformation of the solids was needed due to huge influence by the fluid film thickness when calculating the viscous heating.

The procedure followed in this study is a combination of Vohr [12] and Ettles [14] researches who achieved some methods to approximate the temperature distribution adjusting it with empirical experiments.

The following expression shows the energy equation solved:

$$\underbrace{\rho \cdot C_p \cdot \left(u_f \cdot \frac{\partial T_f}{\partial x} + v_f \cdot \frac{\partial T_f}{\partial y}\right)}_{Q_{convection}} - \underbrace{k \cdot \frac{\partial^2 T_f}{\partial z^2}}_{Q_{conduction}} = \eta \cdot \underbrace{\left[\left(\frac{\partial u_f}{\partial z}\right)^2 + \left(\frac{\partial v_f}{\partial z}\right)^2\right]}_{Q_{shear}} - \underbrace{\frac{T_f}{\rho} \cdot \frac{\partial \rho}{\partial T} \cdot \left(u_f \cdot \frac{\partial p}{\partial x} + v_f \cdot \frac{\partial p}{\partial y}\right)}_{Q_{compression}} \quad (59)$$

The velocity field $(u_f, v_f, w_f)$ found before is now an input. Some of these terms are usually neglected by previous assumptions. In general, the shear source is more important than the compressive one [42]. In this work, all the terms have been taken into account and thus the full equation is included to the model.

Another problem showed up during the modelling procedure. Given the dimensions of the fluid layer it was not possible to mesh it. So there is the need to scale it to be computable.

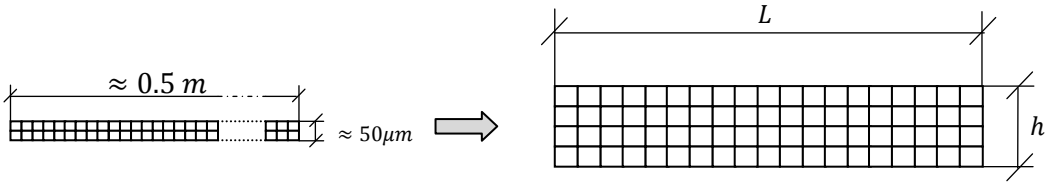


*Figure 24. Scaling procedure scheme.*

$$\bar{H} = {}^{h}/_{h_{red}} = {}^{h}/_{h_{min}} \qquad \bar{p} = {}^{p}/_{p_{red}}$$
$$\bar{X} = {}^{x}/_{x_{red}} = {}^{x}/_{\theta_{ref} \cdot R_{int}} \qquad \bar{T} = {}^{T}/_{T_{red}}$$
$$\bar{Y} = {}^{y}/_{y_{red}} = {}^{y}/_{W} \qquad \bar{\rho} = {}^{\rho}/_{\rho_{red}}$$
$$\bar{Z} = {}^{z}/_{z_{red}} = {}^{z}/_{H_{min}} \qquad \bar{\eta} = {}^{\eta}/_{\eta_{red}}$$

$$\rho C_p \left(u_f \frac{\partial T_f}{\partial x} + v_f \frac{\partial T_f}{\partial y}\right) - k_f \frac{\partial^2 T_f}{\partial z^2} = \eta \left[\left(\frac{\partial u_f}{\partial z}\right)^2 + \left(\frac{\partial v_f}{\partial z}\right)^2\right] - \frac{T_f}{\rho} \frac{\partial \rho}{\partial T_f} \left(u_f \frac{\partial p}{\partial x} + v_f \frac{\partial p}{\partial y}\right)$$

$$\bar{\rho}\rho_{red} C_p \left(u_f \frac{\partial \bar{T}_f T_{red}}{\partial \bar{X} x_{red}} + v_f \frac{\partial \bar{T}_f T_{red}}{\partial \bar{Y} y_{red}}\right) - k_f \frac{\partial^2 \partial \bar{T}_f T_{red}}{\partial \bar{Z} z_{red}^2} =$$
$$= \bar{\eta}\eta_{red} \left[\left(\frac{\partial u_f}{\partial \bar{Z} z_{red}}\right)^2 + \left(\frac{\partial v_f}{\partial \bar{Z} z_{red}}\right)^2\right] - \frac{\bar{T}_f T_{red}}{\bar{\rho}\rho_{red}} \frac{\partial \bar{\rho}\rho_{red}}{\partial \bar{T}_f T_{red}} \left(u_f \frac{\partial \bar{p} p_{red}}{\partial \bar{X} x_{red}} + v_f \frac{\partial \bar{p} p_{red}}{\partial \bar{Y} y_{red}}\right) \quad (60)$$

Studying thoroughly the software it was discovered that the use of quadrangular or mapped elements mesh instead of the free tetrahedral ones makes possible the

computation without the need of scaling it. So the dimensionless equation was not used anymore.

The fluid velocity field $U_f$ is needed to determine the viscous heating as it is seen in *Eq. 61*. The velocity field is obtained following the procedure explained in *4.1.4 Fluid Film Velocity Field* and applying *Eq. 33* and *Eq. 34*.

$$Q_{vh} = \frac{\eta \cdot \nabla U_f + \left(\nabla U_f\right)^T}{\nabla U_f} \qquad (61)$$

As commented, the film thickness is essential to obtain a proper viscous heating; a moving mesh is required to vary the thickness of the fluid model. To define the mesh displacement a deeper insight on the gap variation is depicted in *Figure 25*.

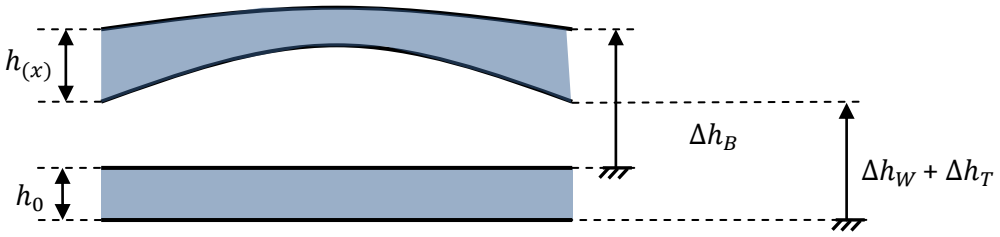


*Figure 25. Fluid film deformation scheme.*

Although it is possible to apply the mesh displacement to achieve the exact gap geometry, the velocity field input assumes a flat lower gap surface. Finally, pad and collar surfaces are assumed flat and the thickness of the fluid model varies with the average deformation of the pad and collar surfaces.

The boundary conditions defined in the fluid model are based on Vohr's research [12]. Vohr proposed a heat balance defining a control volume which includes the entire pad *(Figure 26).* Following this method, it is assumed that the heat transferred out of the control volume must be equal to the power dissipated in the bearing $P_b$.

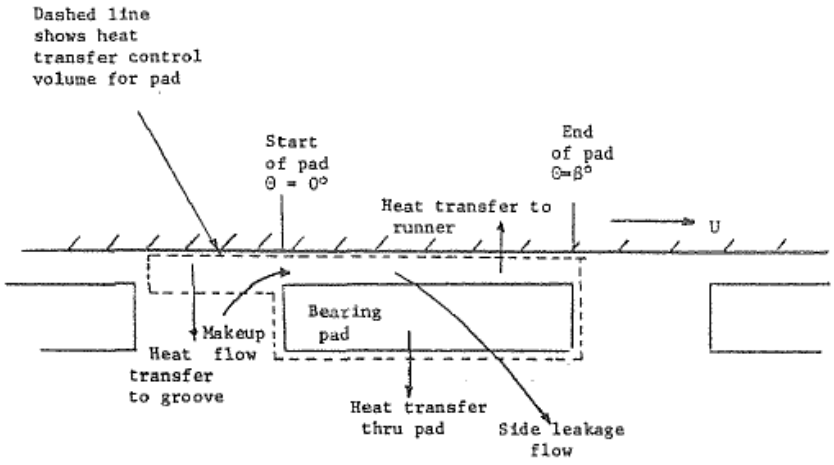


*Figure 26. Control volume of the heat transfer analysis [12].*

The heat fluxes considered in this work are the side leakage $Q_l$, the net heat conducted into runner $Q_r$, the heat transfer through the pads $Q_p$, and finally the heat transferred to cold oil in groove between pads $Q_g$. It is also taken into account the reverse flow swept back by the makeup flow of lubricant entering to the pad. So the losses from the bearing are defined as:

$$Q_l + Q_p + Q_r + Q_g = P_b \quad (62)$$

The convection coefficients defined on Vohr's paper were adjusted to the bearing studied. From Vohr's work is shown the variability of the percentage of each kind of loss dissipated depending on the running conditions [12].

The heat lost by side leakage $Q_l$ is the one transferred by the fluid on a radial displacement $q_r$ entering and leaving the pad though the inner and outer radius. Vohr published the following expression:

$$Q_l = n_{pads} \cdot \rho \cdot C_p \cdot \left[ \int_0^{\beta} q_r(r_0, \theta) \cdot [T(r_0, \theta) - T_b] \cdot r_0 d\theta - \int_0^{\beta} q_r(r_i, \theta) \cdot [T(r_i, \theta) - T_b] \cdot r_i d\theta \right] \quad (63)$$

The expression has two differenced parts. The first one is referred to heat transferred in the fluid flow at the outer edge and the second to the heat transferred through the inner edge. The flow rates are obtained from the pressure following the expressions *Eq. 64* and *Eq. 65*.

$$q_\theta = -\frac{h^3}{12 \cdot \eta} \cdot \frac{1}{r} \cdot \frac{\partial p}{\partial \theta} + \omega \cdot r \cdot \frac{h}{2} \quad (64)$$

$$q_r = -\frac{h^3}{12 \cdot \eta} \cdot \frac{1}{r} \cdot \frac{\partial p}{\partial r} \quad (65)$$

The temperatures in the inner $T(r_i, \theta)$ and outer radius $T(r_o, \theta)$ are obtained by solving the energy equation *(Eq. 59)* in the fluid film model. The bath temperature $T_b$ is a constant boundary condition.

The expression given to calculate the heat transferred through the pad $Q_p$ is convection expression through the pad surface $A_{pad}$:

$$Q_p = H_l \cdot A_{pad} \cdot (T_f - T_b) \quad (66)$$

Vohr defined an average temperature of the pad $T_f$ and a constant bath temperature $T_b$. The overall convection coefficient $H_l$ is calculated using the next expression::

$$H_l = \frac{H_p \cdot k_p / N}{H_p + \frac{k_p}{N}} \quad (67)$$

Being $k_p$ the thermal conductivity of the pad, $N$ is the pad thickness and $H_p$ the pad lower surface heat transfer coefficient. In the model defined, it has been input the overall

coefficient $H_l$. The same procedure is followed to take into account the heat transferred into the runner $Q_r$. An overall convection coefficient was also defined.

The most complex to define is the heat transferred to the cold oil groove between pads $Q_g$. Ettles researched on the lubricant behaviour inside this groove [9] [10]. The study was carried out considering a 2D rectangular gap with a motion top surface performing as the runner and supposing laminar flow. Later, Wasilczuk [30] considered it insufficient and decided to study it in 3D comparing the differences observed. The groove between pads deserves a special consideration because it is responsible to supply and remove the fluid from gap between the pad and the collar. The goal of the grooves is to ensure that the cold lubricant is accurately introduced to replace the already heated oil layer. In the bearing studied, there is no special geometry or supplier to ensure that task so less cold lubricant is input increasing this way the working temperatures. The lack of lubricant replacement is an important problem when working with thrust bearings.

Vohr, approached this problem including this groove in the energy balance: the heat transferred out the control volume *(Figure 26)* must be equal to the power loss in the bearing. He defined a procedure to determine the heat transferred also including the heat picked up by the makeup flow entering the pad. The expression he presented was obtained from empirical experiments and takes into account the runner angular velocity and the pad geometric parameters to determine the proper heat transfer coefficient [12]. The values of that heat transfer coefficient achieved were in the range of 2550 to 3670 $\frac{W/m^2}{K}$.

### 4.3.2 Temperature Distribution of the Solids

To solve the heat transfer equation defined in the solid models, some boundary conditions need to be defined, see *Figure 27*. Using the regression method summarized by Ettles et al. [19], a convection coefficient on the back face of the pad surface is obtained. This coefficient should be matched with some experimental results.

Ettles et al. also defined the relationships between the coefficients for the rest of surfaces. For the inlet, outlet and inner faces it is considered a convection coefficient twice the one used for the back face. The convection coefficient for the outer radius surface of the pad is considered four times the back pad surface one.

The temperature distribution of the lower surfaces from the fluid model is extruded to the pad top surface as a boundary condition, see *Figure 27*.

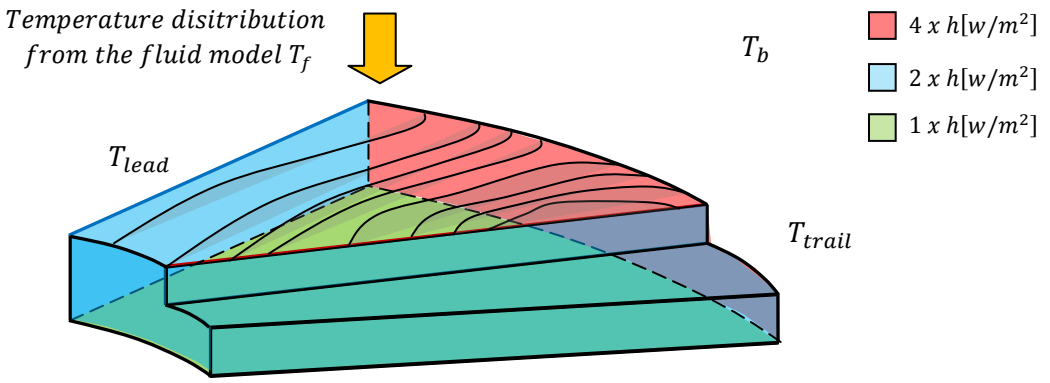


*Figure 27. Boundary conditions applied on the pad to solve the heat transfer equation in the solid.*

Although the temperature distribution on the top part of the fluid $T_r$ which corresponds with the runner is known, do not forget that it is a motion wall so the temperature on the runner is an averaged one. For this reason, the collar lower surface temperature must accomplish:

$$\frac{\partial T}{\partial \theta} = 0; \quad \frac{\partial T}{\partial r} \neq 0; \tag{68}$$

However, Dowson [8] proved that getting the runner temperature $T_r$ from the energy equation was unnecessary because it could be treated isothermally achieving good results.

The temperature of the collar is strongly related with the hot oil carry-over effect. The term "hot oil carry-over" was firstly described by Ettles and Cameron when studied the flow passing across a bearing groove from the trailing edge of one pad to the leading edge of the following one [45]. This effect appears due to the pad-collar relative movement and lubricant viscosity. That phenomenon appears on the grooves between pads when mixing the oil going out from the trailing edge and the oil entering to the leading edge *(Figure 28).*

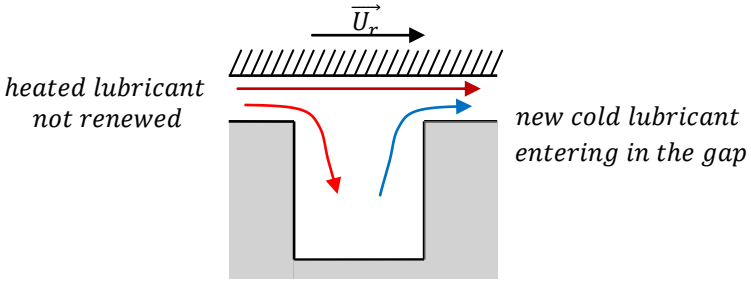


*Figure 28. Hot oil carry-over effect scheme in the groove between pads.*

A simpler way to define the collar uniform temperature is to use an average value from the temperature distribution from the fluid model top surface. This value can be modified to match with experimental results.

Vohr [12] defined a more complex method to determine this uniform temperature on the collar $T_r$. Vohr's procedure assumes that the net heat transferred from the lubricant film to the runner $Q_r$ is equal to the heat transferred from the collar to the lubricant bath.

So the heat from the lubricant is,

$$Q_r = H_u \cdot A_{pad} \cdot (T_f - T_r) \quad (69)$$

And the following expressions obtained from empirical experiments give the heat transferred back from the collar to the lubricant bath,

$$Q_r = U_r \cdot (T_r - T_b) \quad (70)$$

$$U_r = 466 \cdot \left(\frac{r_o + r_i}{2}\right) \quad (71)$$

The heat transfer coefficient $H_u$ is an averaged one between film and runner. An average pad temperature $T_f$ is obtained from the fluid model solution and $A_{pad}$ is the heat transfer surface. The bath temperature $T_b$ is constant and $r_i$ and $r_o$ are collar inner and outer radius. The heat transfer coefficient $H_u$ is an averaged one between film and runner. The value taken is 7.2 based on heat transfer solution between two planes with a middle laminar flow.

Matching *Eq. 70* and *Eq. 71* the collar temperature $T_r$ is obtained as well as the heat transferred into the runner $Q_r$.

Another method to obtain the collar temperature taking into account the hot oil carry-over effect consists in using Ettles' temperature relationships:

$$T_{trail} = T_b + \Delta T \cdot \left(\frac{2 - k_{co}}{2 - 2 \cdot k_{co}}\right) \quad (72)$$

$$k_{co} = \frac{T_{lead} - T_b}{T_r - T_b} \quad (73)$$

$$T_{lead} = T_{trail} - \Delta T \quad (74)$$

Ettles presented a plot [45] where the hot oil carry-over factor $k_{co}$ was obtained from the runner velocity $U_r$. With this factor, the bath temperature $T_b$ and assuming an averaged temperature rise $\Delta T$, the temperature of the leading edge $T_{lead}$, the trailing edge and the collar $T_r$ can be deduced. It was noticed that better approaches can be easily achieved varying softly the $k_{co}$ factor.

The method presented in this paper consists in solving the energy equation *(Eq. 59)* and then using the Ettles' expressions *Eq. 72* and *Eq. 73* to obtain the collar temperature $T_r$. In other words, it is solved the other way around avoiding to apply the uncertain factor $k_{co}$. Since the temperature distribution on the leading and trailing edges obtained from solving the energy equation is not constant, an averaged one needs to be used.

### 4.3.3 Thermal Expansion

All materials suffer a certain expansion or contraction when working at different temperatures. The deformation suffered by iron alloys working on a temperature range between 20ºC and 100ºC is minimal. However, due that the pressure deflections obtained on the pad up to this point are also small, thermal expansion must be considered. Using the temperature distribution, the thermal expansion coefficients from the pad $\alpha_{L_p}$ and the collar $\alpha_{L_r}$ and the *Eq. 75*, the thermal expansion is taken into account.

$$\frac{\Delta L}{L} = \alpha_L \cdot \Delta T \qquad (75)$$

Since allowing pad and collar to be thermally expanded, the problem to deal has been absolutely modified. The material expansion compensates the sagging suffered from the lubricant pressure. Even not having such a large temperature increment, that minimum thermal expansion is enough to partially compensate the sagging produced for the pressure and even produces a deformation on the other way. That phenomenon is shown in *Figure 29* and was baptized by Raimondi as crowning effect [3].

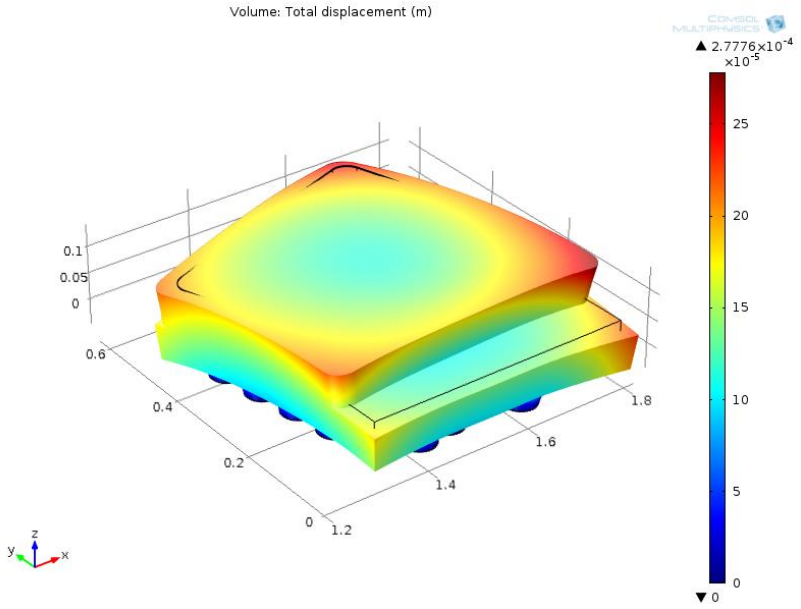


*Figure 29. Displacement of the pad showing the crowning effect due to the combination of fluid pressure and thermal expansion.*

It is important to point out that allowing the pad and collar thermal expansions, the gap geometry becomes easily convergent.

There is no doubt of the importance of considering the thermal effects when working with thrust bearings. Watching the relevance of the thermal expansion, the studies which do not include it are considered doubtful.

The deformation produced confers totally different gap geometry. Depending on the balance between thermal expansion and pressure to bear a particular shape is generated.

Sinha stated that the nature of elastic deformation gives rise to concave surface profile while thermal distortion leads to a concave convex one; the combined effect yields the ultimate profile [21].

It is defined a crowning ratio parameter. It is the quotient between the centre-to-edge deflection $\delta_{def}$ and the minimum film thickness $h_{min}$ . Raimondi stated that crowning up to 1 is shown to be beneficial for offset pivoted pads and essential for centre-pivoted pads [3]. He also ensured that beyond the unity, the capacity decreases sharply with increasing crowning. Ettles also pointed out the relevance of this ratio, ensuring that excessive crowning $\frac{\delta_{def}}{h_{min}} > 2$ tends to give a higher operating temperatures and in crowning over 5 a thermal ratcheting mechanism develops, leading to wiping of the bearings.

The crowning effect must be carefully controlled according to the dimensions of the pads. Small trust pads (< 30mm) must be designed to enforce crowning, particularly if they are centrally pivoted. On large thrust bearings, the deformations must be controlled by large disk inserts, arrangements of supporting beams or by mounting on a nest of springs [19].

The spring pattern has a lot to do with the crowning effect. The edge-to-edge springs extension develops negative elastic crowning and must run sufficiently hot so that is countered by thermal crowning [19]. For thin pads it is recommended an extent of 80% [26] and for great pad thicknesses special arrangements are made to eliminate thermal deformation.

## 4.4 Redefining Assumptions

Up to this point of the study, a pressure and temperature distribution of the entire assembly has been obtained.

It is time to redefine the Reynolds equation used until now where the fluid density and viscosity were considered constants values. From now on, the Reynolds equation used to obtain the pressure distribution on the top surface of the pad reads:

$$\frac{\partial}{\partial x}\left(\frac{\rho h^3}{12\eta}\frac{\partial p}{\partial x}\right)+\frac{\partial}{\partial y}\left(\frac{\rho h^3}{12\eta}\frac{\partial p}{\partial y}\right)=\frac{\partial}{\partial x}\left(\frac{u_r}{2}\left(\frac{\partial(\rho h)}{\partial x}\right)\right)+\frac{\partial}{\partial y}\left(\frac{v_r}{2}\left(\frac{\partial(\rho h)}{\partial y}\right)\right) \quad (76)$$

The density of a fluid varies according to the temperature and pressure in the gap. Due to its larger variation with the temperature it is generally considered only temperature dependant. The expression below is used to take into account the density variation on the thin lubricant film:

$$\rho_1 = \frac{\rho_0}{1 + \beta_f (T_1 - T_0)} \quad (77)$$

So taking a certain density $\rho_0$ at a certain temperature $T_0$ and the volumetric temperature expansion coefficient $\beta_f$ from the material, it is possible to approximate the density $\rho_1$ at the working temperature $T_1$.

It has been possible to take also into account the density variations due to the pressure distribution using the following expression:

$$\rho_1 = \frac{\frac{\rho_0}{1 + \beta_f (T_1 - T_0)}}{1 - \frac{p_1 - p_0}{E_f}} \quad (78)$$

The initial pressure $p_0$ and the bulk modulus $E_f$ have been input. A new final pressure $p_1$ is obtained from the model.

The specific data from the lubricant was provided by the company on charge of the hydroelectric turbine.

From the literature review, the main part of the studies conclude affirming that the viscosity $\eta$ variation due to the temperature $T$ distribution plays an important role when working with thrust bearings, even more when treating with a huge dimensions one.

Some lubricants suffer an important viscosity variation when working at different temperatures. Empirically, it has been proved that different fluids follow specific expressions when the temperature is switched.

Which expression fits better with the defined lubricant behaviour was consulted. The company has done some experiments while testing the lubricant, those where provided and used in this thesis. The proprieties from other lubricants have been also provided in order to test them and get a first prediction of the bearing behaviour.

Generally, it is reasonable to use the Vogel's expression *(Eq. 79)*. It is an empirical relation with minimum deviation from observed variation of viscosity with temperature [33]. From two viscosity measurements at two different temperatures, the expression can be adjusted:

$$\eta = e^{\left(A + \frac{B}{T}\right)} \quad (79)$$

Every lubricant has a working temperature range limited for its freezing point and its flash point. Even the proprieties of the lubricant will vary between these two temperatures it is important to avoid running close to the border temperatures. The oil required in a thrust bearing generally can bear working temperatures from -35ºC to 210ºC. So, even with high rotation velocities it is difficult to achieve these temperatures. Lubricant ageing is another factor taken into account when choosing thrust bearing oil. This phenomenon has not been studied in this study.

The rest of the material proprieties are also linked with the temperature of the nodes using the default expressions of the software.

# 5 Results and Discussion

A model to predict the behaviour of spring-supported thrust bearings has been developed. The doubt over the capability of developing a FEM model to predict the working conditions of a thrust bearing has been overcome. The model works fine coupling accurately the phenomena conditioning the definition of the Reynolds equation. The pressure phenomenon has been deeply studied and therefore the approach obtained has into account the main parameters involved. High attention is paid to the gap geometry due to its important role when working with the Reynolds equation. The final model is capable to combine the pad and runner displacement fields to perfectly define the final gap morphology. These displacement fields from the solid compounds take into account the deflection caused by the pressure developed and the thermal expansion which actually counteracts the elastic deflection.

The model predicts a temperature distribution on the entire assembly solving the energy equation inside the fluid domain and via a heat transfer balance with the solids representing the pad and collar. When calculating the viscous heating, the velocity field defined is simplified; ideally a velocity profile considering the final gap geometry, side leakages, reverse flows, laminar-turbulent phase and cavitation should be implemented. However, due to the uncertainties assumed when defining the heat transfer boundary conditions, it would be pointless to define a better velocity profile. The boundary conditions have been obtained from other studies and, obviously, are just approximations.

The model has been developed for hydrodynamic conditions; no hydrostatic elements have been considered.

The material properties have been found playing an important role. Although the most part of them have been well defined, the Babbitt material proprieties are uncertain. Some studies proofed that the Babbitt can significantly influence the range of operating temperatures [46].

The model has been implemented so it may be easily adapted for similar ype of applications. *Table 1* lists all the input variables required for the simulation. The values defined for each parameter are taken from different studies. i.e., the ones published by Ettles [13] and Ferguson [23].

| | | | | | |
|---|---|---|---|---|---|
| **Working Conditions** | | | | | |
| | Turbine Angular Speed | | n | 100 | [$min^{-1}$] |
| | External Load | | Wext | 1 | [MN] |
| | Pad Weight | | Mpad | 250 | Kg |
| | Bath Temperature | | Ttank | 40 | [ºC] |
| **Geometry Parameters** | | | | | |
| | Pad Outer Radius | | Rext | 1750 | [mm] |
| | Pad Inner Radius | | Rint | 1250 | [mm] |
| | Pad Base Angle | | alphap | 20 | [ºC] |
| | Pad Base Height | | hp | 60 | [mm] |
| | Pad Step Angle | | alphas | 3 | [ºC] |
| | Pad Step Height | | ht | 60 | [mm] |
| | Babbitt Thickness | | hb | 3 | [mm] |
| | Fillet Radius | | Rfillets | 25 | [mm] |
| | Number of pads | | npads | 18 | [u] |
| | Collar/Runner Thickness | | hr | 150 | [mm] |
| **Materials Proprieties** | | | | | |
| | **Pad** | | | | |
| | | Density | rho | 7850 | [$Kg/m^3$] |
| | | Young Modulus | E | 207 | [GPa] |
| | | Poisson Ratio | nu | 0.3 | [ ] |
| | | Thermal Conductivity | alpha | 52 | [W/m] |
| | | Coefficient of Thermal Expansion | k | $1{,}1 \cdot 10^{-5}$ | [1/K] |
| | | Heat Capacity at Constant Pressure | Cp | 475 | [J/kg*K] |
| | **Babbitt** | | | | |
| | | Density | rho | 7850 | [$Kg/m^3$] |
| | | Young Modulus | E | 207 | [GPa] |
| | | Poisson Ratio | nu | 0.3 | [] |
| | | Thermal Conductivity | alpha | 52 | [W/m] |
| | | Coefficient of Thermal Expansion | k | $1{,}1 \cdot 10^{-5}$ | [1/K] |
| | | Heat Capacity at Constant Pressure | Cp | 475 | [J/kg*K] |
| | **Collar** | | | | |
| | | Density | rho | 7850 | [$Kg/m^3$] |
| | | Young Modulus | E | 207 | [GPa] |
| | | Poisson Ratio | nu | 0.3 | [] |
| | | Thermal Conductivity | alpha | 52 | [W/m] |
| | | Coefficient of Thermal Expansion | k | $1{,}1 \cdot 10^{-5}$ | [1/K] |
| | | Heat Capacity at Constant Pressure | Cp | 475 | [J/kg*K] |
| | **Fluid** | | | | |
| | | Dynamics Viscosity | mu | | [Pa·s] |
| | | Density | rho | 890 | [$Kg/m^3$] |
| | | Heat Capacity at Constant Pressure | Cp | 1880 | [J/Kg·K] |
| | | Thermal Conductivity | alpha | 0,15 | [W/m·K] |
| | | Ratio of specific Heats | gamma | 1,87 | [ ] |

| **Springs Mattress** *(Specific springs distribution defined. It can be adapted to each case)* | | | | |
|---|---|---|---|---|
| | Springs Elastic Constant | k | $152 \cdot 10^{-3}$ | MN/m |
| | Springs separation (y-direction) | a | 80 | [mm] |
| | Springs separation (x-direction) | b | 65 | [mm] |
| | Spring radial reference | Sx0 | 1300 | [mm] |
| | Springs Compressed Longitude | $l_0 - \Delta l$ | 50 | [mm] |
| | Springs Diameter | Dspring | 30 | [mm] |

*Table 2. Data required for the simulation.*

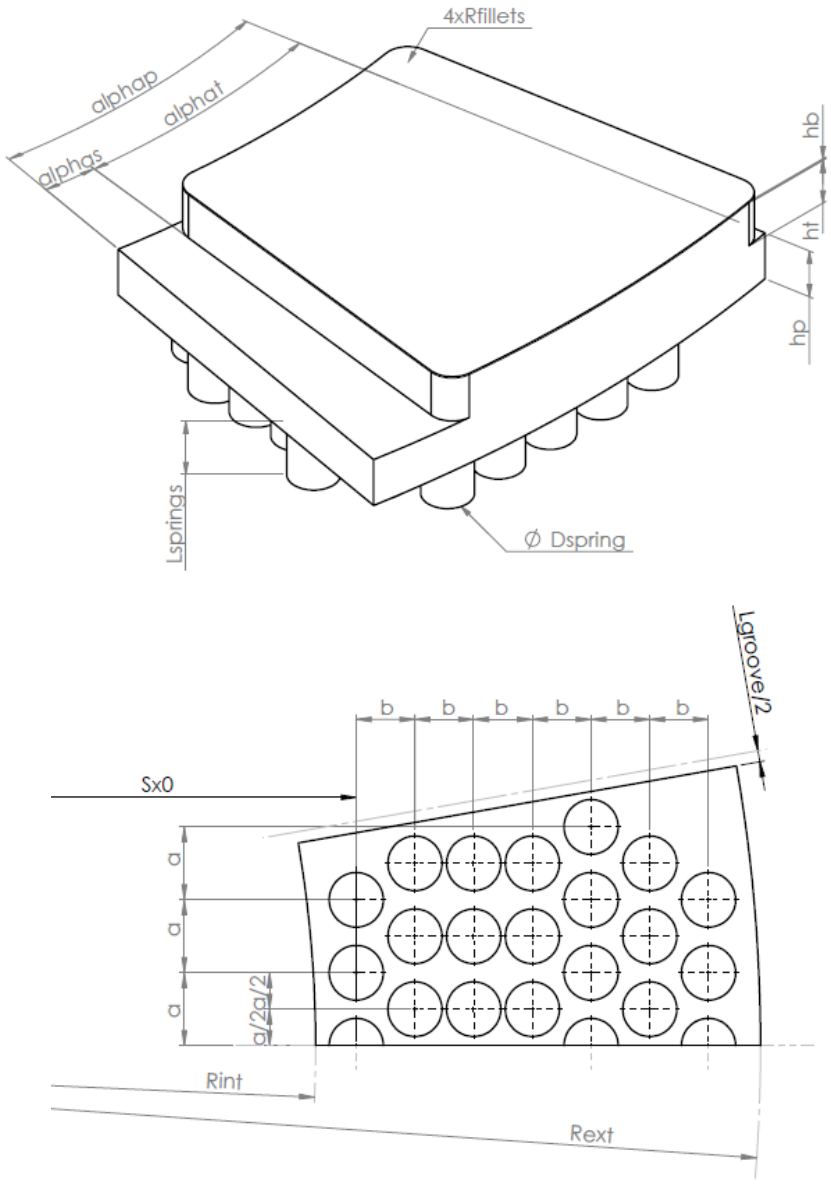


*Figure 30. Scheme with the necessary inputs for simulating the model.*

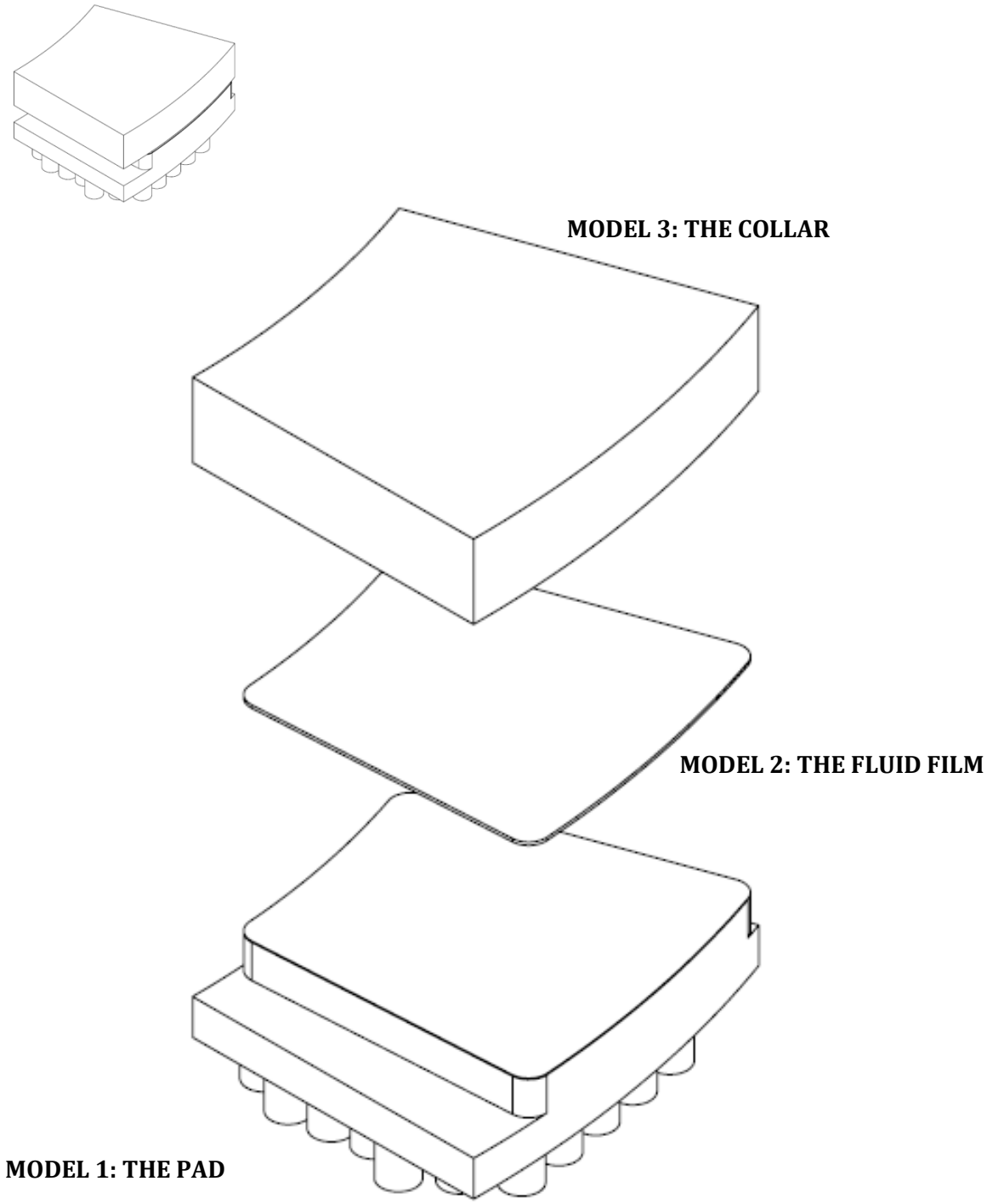


*Figure 31. Final model representation.*

| MODEL COUPLING | | | TO | | | | | | |
|---|---|---|---|---|---|---|---|---|---|
| | | | Pad | | | Fluid | | Collar | |
| | | | LS | SM | HTs | MM | HTf | SM | HTs |
| FROM | Pad | LS | | pf | | | pf | pf | |
| | | SM | u,v,w | | X,Y,Z | u,v,w | | | |
| | | $HT_s$ | | T | | | | | |
| | Fluid | MM | | | | | X,Y,Z | | |
| | | $HT_f$ | | | T | | | | T |
| | Collar | SM | u,v,w | | | u,v,w | | | X,Y,Z |
| | | HTs | | | | | | T | |

| Physics: | |
|---|---|
| LS | Lubricant Shell |
| SM | Solid Mechanics |
| $HT_s$ | Heat Transfer in Solids |
| MM | Moving Mesh |
| $HT_f$ | Heat Transfer in Fluids |

| Variables: | |
|---|---|
| pf | Fluid Pressure |
| u, v, w | Displacement Field |
| X, Y, Z | New Coordinates System |
| T | Temp Distribution |

*Table 3. Model coupling scheme.*

The model predicts the pressure applied on the pad, the deformation suffered from pad and collar, the film thickness and the temperature distribution under a wide range of operating conditions.

## 5.1 Considering a Rigid Collar

The most part of the available papers published do not take into account the deformation of the collar. The common way to deal with it is either assuming zero displacement or equal deformation of the pad and the collar even though the pad and collar materials are usually different.

In the present thesis it has been necessary to model the collar separately. A substantial computational effort is needed considering both surfaces separately. However, the importance of taking the collar deformation into account or not can this way be assessed.

## 5.2 Thermal Effects

A significant difference was found when including the thermal expansion in the simulations. Thermal expansion leads to a crowning effect encountered by both surfaces, which in turn give rise to totally different gap morphology. Most papers do not consider thermal expansion in their calculations. It is important to point out the difficulties of achieving a convergent gap profile when simulating without considering the thermal deformation.

## 5.3 Considering different Fluid Proprieties

When there is the desire of modifying the turbine performance, the easiest (least expensive) way of doing it, is changing the lubricant. Disassemble a turbine from a hydroelectric energy plant represents a significant cost. Therefore the companies in charge spend a lot of research on finding more efficient lubricants.

## 5.4 Influence of varying the External Load

The load supported by the thrust bearing is obviously a determining parameter. The bearing has to be able to support the weight of the shaft. The weight of the shaft is constant; however, the amount of water going in and out of the turbine is not. The model developed has the external load as a constant input. The load support generated by the pressure distribution must of course be equal to the external load. This requires the addition of a force-balance equation to the model. Remember that the model only represents one pad segment, the total shaft weight plus the water load must be divided by the number of pads forming the thrust bearing.

In the *Figure 32*, *Figure 33* and *Figure 34* are shown the effects of varying the external load on the main output variables. The rotational velocity of the shaft has been kept constant to 100 $min^{-1}$.

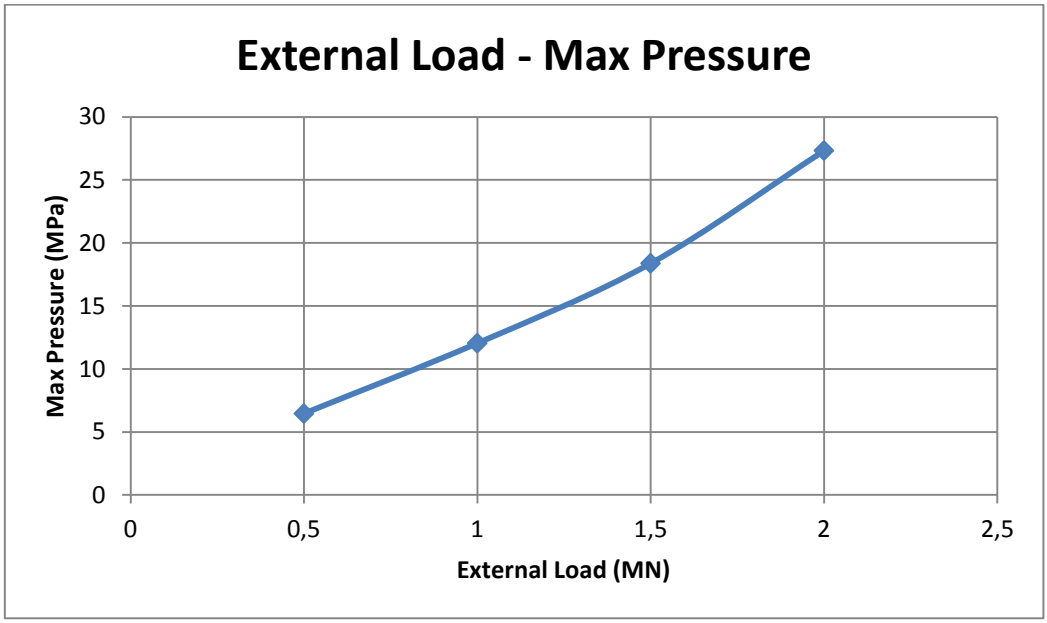


*Figure 32. Load Variation - Maximum Pressure on the Gap.*

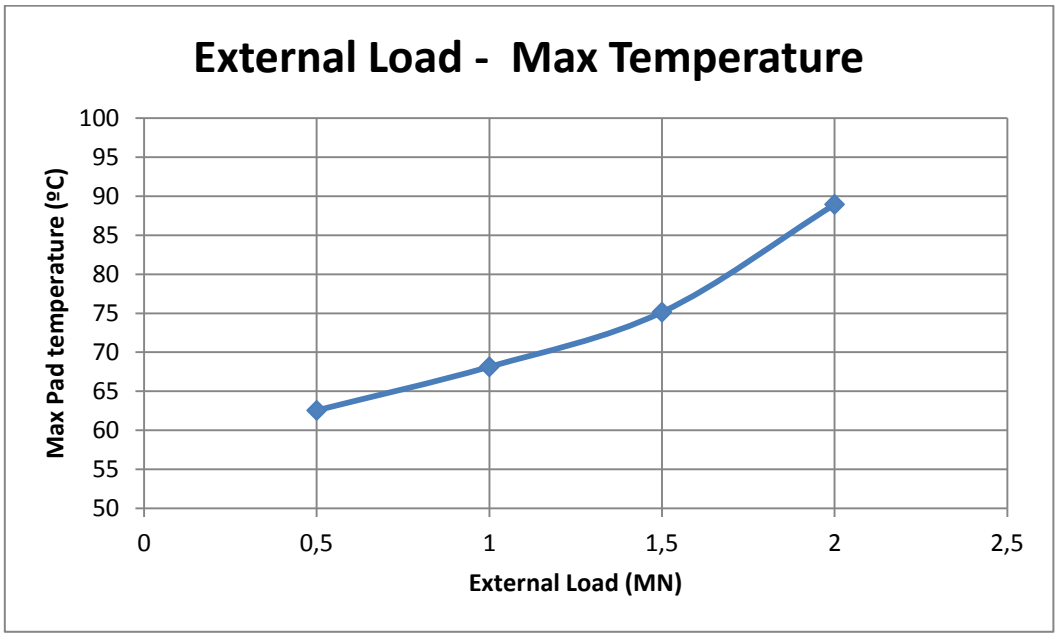


*Figure 33. Load Variation - Maximum Temperature on the Pad.*

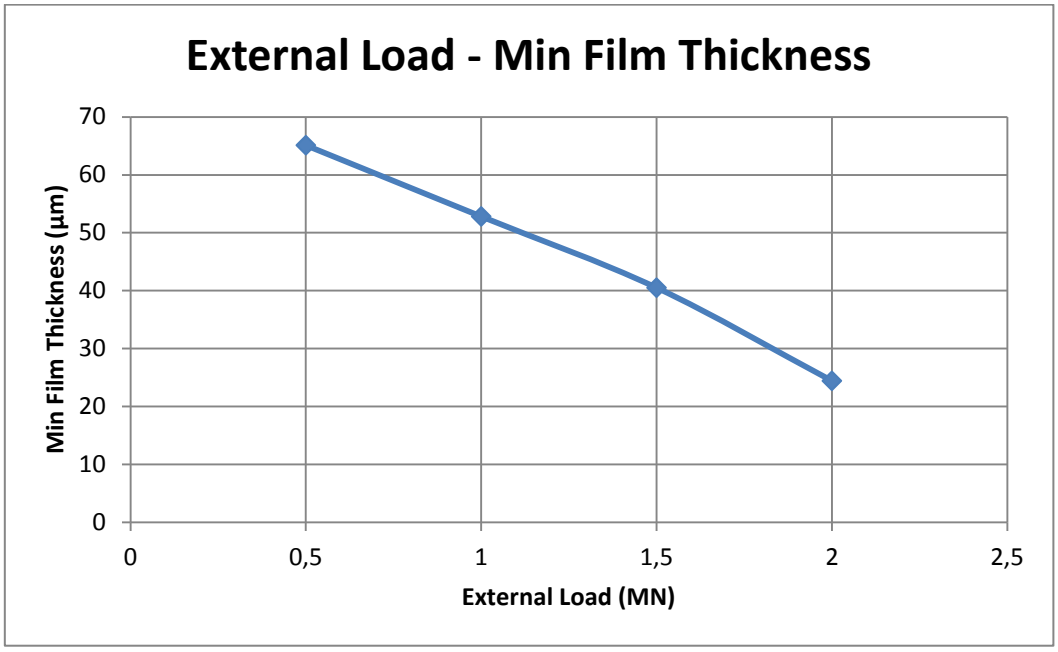


*Figure 34. Load Variation - Minimum Film Thickness.*

When working with thrust bearings, the minimum film thickness is an important design parameter. It is considered very dangerous to run turbines with a film thickness below 15 micrometers.

## 5.5 Collar Preload Deformation

The drawings provided by the company in charge of the turbine marks out the positions of the screws joining the collar and the shaft. These screws probably play an important role when defining the initial geometry of the collar. Theoretically, the collar surface should be flat however it is not due to the compression of the screws. The collar shape is affected by this preload suffering a pre-bending before any load is applied. The company in charge is aware of this fact and some measurements of that pre-deformation have already been done.

In order to figure out which role this phenomenon plays and its importance under normal working conditions, the collar geometry has been modified *(( 81)*. The initial shape has been defined in function of a unique parameter *(s)* representing the highest distance between the flat surface and the deflected one (*Figure 35*).

$$y_0 = f(s) \quad R = f(s) \tag{80}$$

$$R = \frac{\left(r_o - \frac{r_i + r_o}{2}\right)^2 + s^2}{2 \cdot s} \tag{81}$$

$$y_0 = -R + s \tag{82}$$

$$x_0 = \frac{r_i + r_o}{2} \tag{83}$$

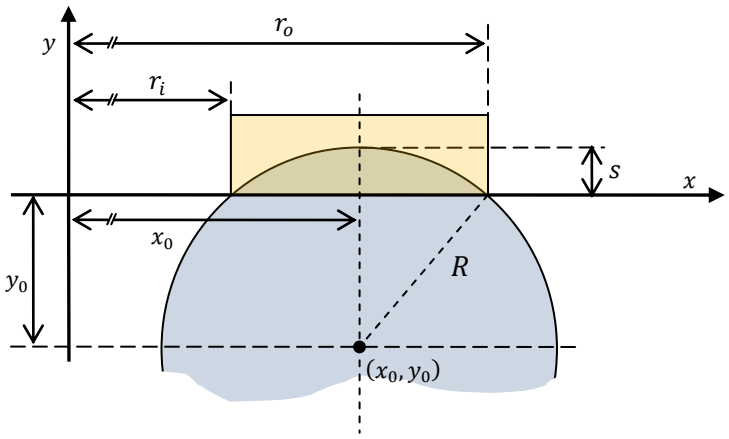


*Figure 35. Collar deformation scheme from the mathematical approximation used.*

# 6 Concluding Remark

The performance of a thrust bearing relies on the balance between elastic deformation and thermal crowning of both pad and collar surfaces. These two phenomena define the geometry of the gap. Other parameters, such as the pattern of spring mattress, spring stiffness, the choice of the proper materials and the pad geometry simply makes it easier to obtain good gap geometry for a wider range of operating conditions. The use of FEM to approach this complex PDE system has proved to be useful and that it lends itself to conveniently include a number of different physics and couple different, even solution based computational domains. The most uncertain part in the simulation of thrust bearing performance, is predicting the temperature distribution. There are also uncertainties in how to govern the fluid flow. The fluid velocity field plays an essential role in the energy equation and highly influences the prediction of temperature distribution. It is also difficult to define appropriate heat transfer coefficients. For all these reasons, all the studies rely on backwards engineering adapting coefficients in the governing equations to match the solutions against experimental data.

# 7 Future Work

A model can always be improved in order to obtain greater accuracy of its predictions.

In the present work, the fluid is considered as being laminar, which probably is an assumption that is violated in the subsets of the parameter space covered by the simulations. It is known that the fluid flow may turn turbulent at different locations within the fluid film, modifying in this way the flow. The turbulent heat transfer coefficient is greater than the laminar one, and the prediction of pad surface temperatures would be lower if the value for turbulent flow is adopted, especially on the leading edge where the film is thickest [35]. In some sense, this means that the present way of modelling the flow as laminar consists a worst case scenario.

In order to calculate a more accurate temperature distribution the thickness of the lubricant layer was varied to investigate its influence on the results. Heat transfer coefficients have been adjusted to match with experimental results assuming an averaged film thickness variation depending on pad and runner deformation. Although the software is able to do it, when describing the velocity field it does not converge to any solution. In addition the velocity field is defined considering the pad and the runner flat surfaces. The velocity is obtained directly from solving the Reynolds equation.

Thorough research must be conducted to acquire better estimates of the material proprieties. The Babbitt plays a positive role, however, the variation of the parameters describing the material with different running conditions of the bearing are not fully understood. As it has been stated by many authors, the morphology and the Babbitt material can decrease the temperature distribution within the fluid film and on the surfaces and inside the material of the pad and collar, greatly influencing the bearing performance, see e.g. [14] and [47].

The collar is constantly rotating at the turbine shaft angular velocity. For this reason, it cannot be treated as a fixed pad. The temperature distribution should be axisymmetric. This is represented here by assuming a uniform runner surface temperature.

Some experimental results could have helped solving some of the inaccuracies commented. The lack of specific information has been overcome using data from already published studies.

The model has been created in a parameterized manner, so that it easy can be adapted to simulate the performance if various spring-supported step thrust bearings. The next stage in the study would be to add the proper modifications to the model in order to match the results with the experimental data available.

# 8 References

[1] Karassik and J. Igor, Pump handbook, McGraw-Hill, 1986.

[2] G. Liao, "Mounting and running of springs-supported thrust bearings.," *Hubei Elect Technol,* pp. 1-2: 74-76, 1994.

[3] A. S. Raimondi, "The influence of transverse and longitudinal profile on the load capacity of pivoted pad bearings," *ASME,* vol. 3, p. 265, 1960.

[4] O. Reynolds, "On the theory of lubrication and its application to Mr Tower's.," *ASME,* vol. 3, p. 265, 1960.

[5] B. Sternlicht and N. Y. Schenectady, "Functional bearings," *United States Patent Office,* 1957.

[6] O. Zienkiewicz, "Temperature distribution within lubricating films between parallel bearing surfaces and its effects on the pressure developed.," *Proc. Conf. on Lubrication and Wear,* pp. 1-7, 1957.

[7] H. Rothbar, "Mechanical designa and systems handbook.," *McGraw-Hill,* 1964.

[8] D. Dowson, J. D. Hudson, B. Hunter and C. N. March, "Proc. Instn. Mech. Engrs.," *181,* p. 70–75, 1966–1967.

[9] C. M. Ettles and A. Cameron, "Solutions for Flow in a Bearing Groove.," *Proceedings of the Institution of Mechanical Engineers,* no. 182, pp. 120-131, 1967.

[10] C. M. Ettles and A. Cameron, "Consideration of flow across a bearing groove.," *Journal of Lubrication Technology,* vol. 90, p. 312, 1968.

[11] V. Castelli and S. B. Malanoski, "Method for solution of lubrication problems with temperature and elasticity effects; application to sector , tilting-pad bearings.," *ASME Journ. Lub. Tech.,* no. 91, pp. 634-640, 1969.

[12] J. H. Vohr, "Prediction of operating temperature of thrust bearings.," *ASME,* vol. 103, pp. 97-106, 1981.

[13] C. M. Ettles, "Transient thermoelastic effects in fluid film bearings.," *Wear,* p. Vol.79 53 – 71, 1982.

[14] C. M. Ettles, "Three dimensional computation of thrust bearings.," *Tribology Series,* pp. Volume 11, Issue C, Pages 95-104., 1987.

[15] H. Heshmat and O. Pinkus, "Analysis of starved journal bearings including temperature and cavitation effects.," *Journal of Tribology,* vol. 107, no. 1, 1985.

[16] Dimarogonas and D. Andrew, Computer aided machine design., California: Prentice Hall, 1989.

[17] P. L. Jiang and L. Yu, "Effect of a hydrodynamic thrust bearing on the statics and dynamics of a rotor-bearing system," *Mechanics Research Communications,* vol. 25, no. 2, pp. 19-244, 1998.

[18] N. Mittwollen and J. Glienicke, "Operating conditions of multi-lobe journal bearings under high thermal loads.," *J. Trib.,* vol. 112, p. 330, 1990.

[19] C. M. Ettles, "Some factors affecting the design of spring supported thrust bearings in hydroelectric generators.," *J. Tribology, Trans. ASME,* pp. 112, 626-632., 1991.

[20] N. M. Ashour, K. Athre, Y. Nath and S. Biswas, "Elastic distortion of large thrust pad on an elastic support.," *Tribology International,* 1991.

[21] A. N. Sinha, K. Athre and S. Biswas, "Spring-supported hydrodynamic thrust bearing with special reference to elastic distortion analysis.," *Tribology International,* 1993.

[22] W. G. Willis, "Tilting Pad Thrust Bearings Tests – Influence of Oil Flow Rate on Power Loss Temperatures.," *Tribology of Energy Conservation,* 1998.

[23] J. H. Ferguson, J. H. Yuan and J. B. Medley, "Spring-supported thrust bearings for hydroelectric generators: Influence of Oil Viscosiy and Power Loss.," *Tribology Series,* pp. 187-193, 1998.

[24] Xiaojing and Wang, "Improving the performance of spring-supported thrust bearings by controlling its deformations.," *Tribology International,* 1999.

[25] S. Eskild, "Dynamic characteristics of hydrodynamically lubricated fixed-pad thrust bearings.," *Wear 232,* pp. 250-255, 1999.

[26] A. L. Brown, J. H. Ferguson and J. B. Medley, "Spring-supported thrust bearings for hydroelectric generators: Finite element analysis of pad deflection.," *Tribology Series,* vol. 39, pp. 99-110, 2001.

[27] S. G. Glavatskih, Ö. Uusitalo and D. J. Spohn, "Simultaneous monitoring of oil film thickness and temperature in fluid film bearings.," *Tribology International,* vol. 34, pp. 853-857, 2001.

[28] A. K. Osman, "Analysis of a hydrodynamic thrust bearing with elastic deformation using a recurrent neural network.," *Tribology International,* 2002.

[29] D. Markin, D. M. C. McCarthy and S. B. Glavatskih, "A FEM approach to simulation of tilting-pad thrust bearing assemblies.," *Tribology International,* 2003.

[30] M. Wasilczuk and G. Rotta, "Modeling lubricant flow between thrust bearing pads.," *Tribology International,* vol. 42, pp. 908-913, 2008.

[31] E. Güllü, "The effects of bearing distortion on the performance of hydrodynamic thrust bearings.," *Industrial Lubrication and Tribology,* vol. 57, no. 3, pp. 121-127, 2005.

[32] Gultekin and W. Karadere, "The effects of the total bearing deformation on the performance of hydrodynamic thrust bearings.," *Industrial Lubrication and Tribology,* 2010.

[33] D. V. Srikanth, "Determination of a large tilting pad thrust bearing angular stiffness.," *Tribology International,* 2011.

[34] D. J. Song and D. K. Seo, "A Comparison Study Between Navier-Stokes Equation and Reynolds Equation in Lubricating Flow Regime.," *KSME International Journal,* pp. Vol 17 No. 4, pp. 599-605, 2003.

[35] M. Tanaka, "Recent thermohydrodynamic analyses and designs of thick-film bearings.," *Journal of Engineering Tribology,* vol. 214, no. 1, pp. 107-122, 2000.

[36] J. Bernard, Hamrock, R. Steven, B. Schmif and O. Jacobson, "Fundamentals of Fluid Film Lubrication.," 2004.

[37] G. Batchelor, "An introduction to fluid mechanics.," *Cambridge University Press,* pp. Pages 14-16, 1967.

[38] Szeri and Z. Andras, Fluid Film Lubrication, New York: Cambridge University Press, 1998, 2011.

[39] Moholkar, S. Vijayanand, Pandit, A. B and AIChe, "Bubble Behaviour in Hydrodynamic Cavitation: Effect of Turbulence," *Journal,* vol. 43, no. 6, p. 1641–1648, 1997.

[40] R. A. Boudry, E. C. Khun and W. W. Wise, "Influence of load and thermal distortion on the design of large thrust bearings.," *Trans ASME,* pp. 80, 807-818, 1958.

[41] H. Dormois, N. Fillot, P. Vergnea, G. Dalmaz, M. Querry, E. Ioannides and G. E. Morales-Espejela, "First traction results of high spinning large-size circular EHD contacts from a new test rig: tribogyr.," *Tribology Transactions,* vol. 52, no. 2, pp. 171-179, 2009.

[42] W. Habchi, D. Eyheramendy, S. Bair, P. Vergne and G. Morales-Espejel, "Thermal Elastohydrodynamic Lubrication of Point Contacts Using a Newtonian/Generalized Newtoninan Lubricant.," *Tribol Lett,* 2008.

[43] W. Habchi, P. Vergne, N. Fillot, S. Bair and G. Morales-Espeje, "Influence of pressure and temperature dependence of thermal properties of a lubricant on the behavior of circular TEHD contacts.," *Tribology International,* vol. 43, pp. 1842-1850, 2010.

[44] A. K. Tieu, "A numerical simulation of finite-width thrust bearings, taking into account viscosity variation with tempearture and pressure.," *J. Mech. Eng. Sci.,* no. 17, p. 1, 1975.

[45] C. M. Ettles, "Hot oil carry-over in thrust bearings.," *Proceedings of the Institution of Mechanical Engineers,* vol. 184, no. 12, pp. 75-81, 1969.

[46] M. C. Donald McCarthy, "Sliding Bearings for Hydropower Applications – Novel Materials, Surface Texture and EALs.," *Luleå University of Technology,* 2008.

[47] D. M. M. Carthy, Sliding Bearings for Hydropower Applications - Novel Materials. Surface Texture and EALs., Luleå: Luleå Univeristy of Technology: Doctoral Thesis, 2008.

[48] S. Gynt, "Recent development of bearing lubricant systems for vertical generators.," *Allmana Svenska Elektrisha AB Journal Vasteras,* vol. 20, pp. 72-87., 1947.

[49] S. Garg, Y. Nath, K. Athre and S. Biswas, "A new approach to evaluate the defelction of thrust pas on elastic support.," *Tribology International,* vol. 28, no. 7, pp. 439-444, 1995.

[50] T. G. Rajaswamy, T. M. Rao and B. S. Prabhu, "An experimental study sector-pad thrust bearings and evaluation of their thermal characteristics.," *Tribology Series,* vol. 11, p. 121–128., 1987.

[51] N. M. Ashour, "An investigation on large thrust bearings.," *Military Technical College Kobry Elkobbah,* 2009.